Journal of Low Temperature Physics, Vol. 84, Nos. 1/2, 1991

The Magnetic Instability in the Heavy Fermion Compounds $Ce_{1-x}La_xRu_2Si_2$

R. A. Fisher, C. Marcenat,* and N. E. Phillips

Materials and Chemical Sciences Division, Lawrence Berkeley Laboratory, Berkeley, California

and

P. Haen, F. Lapierre, P. Lejay, and J. Flouquet*

Centre de Recherches sur les Trés Basses Températures,† CNRS, Grenoble, France

and

J. Voiron

Laboratoire Louis Néel,† CNRS, Grenoble, France

(Received March 21, 1991)

The magnetization and the specific heat of $Ce_{1-x}La_xRu_2Si_2$ with $x \leq 0.13$ are reported with special attention to the effect of magnetic field and the role of lanthanum doping. Evidence is given of differences between the undoped ($x = 0$) and the solid solution ($x \neq 0$) cases. A common feature is the occurrence of well-defined anomalies in the magnetization at the "metamagnetic" field H_M independently of whether the ground state is one of long-range order or Pauli paramagnetism. For $x = 0$, the ground state appears to be a Pauli paramagnet for any strength of the magnetic field; quantum fluctuations or deviations from an ideal lattice may prevent the occurrence of a true static magnetic transition.

1. INTRODUCTION

Heavy-fermion compounds are examples of highly correlated systems, the study of which can provide keys for the understanding of the link between

*Present address: S.B.T., Dept. Rech. Fond., C.E.N.G., B.P. 85X-38041 Grenoble-Cedex, France.
†Laboratoire associé à l'Université Joseph Fourier, Grenoble.

0022-2291/91/0700-0049$06.50/0

the dynamics of the particles, their magnetism, and their superconducting pairing. The compound $CeRu_2Si_2$ is a particularly interesting case of such interacting heavy fermions, since it is located at the borderline of the magnetic instability between long-range ordering and Pauli paramagnetism. The absence of superconductivity, at least down to 20 mK, allows the observation of the properties of its normal phase down to very low temperatures. It has been extensively studied by macroscopic[1-3] and also microscopic measurements[4] since large single crystals can be produced. For example, it is possible to compare thermodynamic (magnetization M, specific heat C) and transport properties with elastic and inelastic neutron experiments. These studies have shown dramatic changes in the electronic and magnetic properties of $CeRu_2Si_2$ with the applied magnetic field H.[1] Furthermore, they have demonstrated the high sensitivity of this compound to volume changes, i.e., to pressure P.[2-3] The possibility of modifying the properties by the external variables P and H provides an opportunity to change the interactions between particles and thus to understand the origin of the large mass enhancement in heavy-fermion compounds.

The strong dependence of the properties on P and H is due to the fact that $CeRu_2Si_2$ is a Pauli paramagnet (PP) down to 0 K[1] but that modulated antiferromagnetic (AF) order appears in $Ce_{1-x}La_xRu_2Si_2$ alloys for $x \geq 0.08$,[5] and to the occurrence of competing intersite interactions and local fluctuations. There is an increase of the differential susceptibility $[\chi(H) \equiv (\partial M/\partial H)_T]$ with H (seen even in polycrystalline samples[6,7]) followed by a large maximum $\chi(H_M)$ at a field H_M referred to as the metamagnetic field.[1,8] This occurs even in PP $Ce_{1-x}La_xRu_2Si_2$ alloys ($x < 0.08$).[8] For $x = 0$, $H_M(T \to 0)$ is equal to 7.7 T.[9] There is also the occurrence of classical metamagnetic transitions in AF alloys ($x \geq 0.1$).[8]

Recent experimental work also shows an increase of the electronic collision time in elastic and inelastic processes[1] as H approaches H_M; a huge increase of $\chi(H)$ as H approaches H_M and a very high value of the ratio $\chi(H_M)/\chi(0)$; by comparison, a weaker increase in the coefficient of the "linear" term in the specific heat γ and a lower value of the ratio $\gamma(H_M)/\gamma(0)$[10]; a collapse of the observed antiferromagnetic correlations at H_M[4]; and spectacular effects in magnetostriction[9,11] and sound velocity.[3,12] Until now only specific-heat measurements performed, on polycrystalline samples were reported: on $Ce_{1-x}La_xRu_2Si_2$ alloys in zero field between 1.5 and 100 K[7], for $x = 0$ and $H = 0$ at low temperatures ($0.3 < T \leq 1.5$ K)[13,14] and as a function of H at 1.5 K.[15]

Magnetization, magnetic-susceptibility, and specific-heat measurements on single crystals in magnetic fields are reported here. The focus is on the similarities and differences between AF and PP compounds, i.e., on the change due either to the nature of the ground state or to the breakdown of

the translation invariance of the lattice by doping. This study offers the possibility of comparing the properties of well-characterized samples with those of other heavy-fermion compounds for which such extensive studies have not been realized. The dependence of the specific-heat anomaly at the Néel temperature on the proximity to the magnetic instability, i.e., for example, on the values of T_N or on the sublattice magnetization is determined. For PP ground states, the doping with La seems to have a drastic smoothing effect on the anomalies observed in $\chi(H)$ and in C. It is strongly emphasized that, by contrast, pure $CeRu_2Si_2$ would reach almost a true phase transition just at H_M for $T \to 0$.

2. EXPERIMENTAL DETAILS

The single crystals of $Ce_{1-x}La_xRu_2Si_2$ ($x=0$, 0.05, 0.1, and 0.13) used in the present study were prepared as described in previous publications.[1–5,8–12]. Polycrystalline ingots were first obtained by melting elements of nominal purity 4N for Ce and 5N for Ru and Si in an induction furnace. Single-crystal rods were then grown from these ingots by the Czochralsky technique in a three-arc furnace. All operations were carried out under a purified argon atmosphere. The alloy crystal with $x=0.13$ is the same as that used previously[5] for neutron-diffraction experiments. The specific-heat measurements were performed by a heat-pulse method. They extend from 0.1 to $\sim$30 K for $H=0$ and from 0.4 to $\sim$30 K in magnetic fields to 7.5 T. The field was applied along the c direction of the tetragonal structure.

Magnetic measurements were made either on the same crystals or on parts of them, depending on their initial size. Most of these measurements were made in fields up to 7.5 T, between 1.5 K and room temperature, by an extraction method; two or three extractions were used in some cases in order to increase the accuracy of the data. Magnetization measurements were done also at 1.4 and 4.2 K up to 15 or 20 T at the Service National des Champs Intenses (SNCI, CNRS, Grenoble). In all magnetization measurements, the magnetic field was also applied parallel to the c axis. The reproducibility between different experiments is better than 1%. The differential susceptibilities $\chi(H)$ were calculated by taking the derivative of the M versus H curves; this was done for each $M(H)$ data point by fitting a quadratic function to this point and its two neighbors and then taking the derivative of this function. The initial susceptibilities [$\chi(0)$] are defined as the low-field, independent-of-H values of $\chi(H)$ (corresponding to linear variations of M versus H, with, in some cases, the neglect of the data points taken at the lowest fields, below 0.1 and 0.3 T, when their accuracy was considered insufficient).

3. MAGNETIZATION

3.1. Initial Susceptibility

Figure 1 shows the inverse of the low-field susceptibility along the easy c axis as a function of temperature for $CeRu_2Si_2$ and the three lanthanum doped samples. For each of the latter, the vertical scale has been displaced

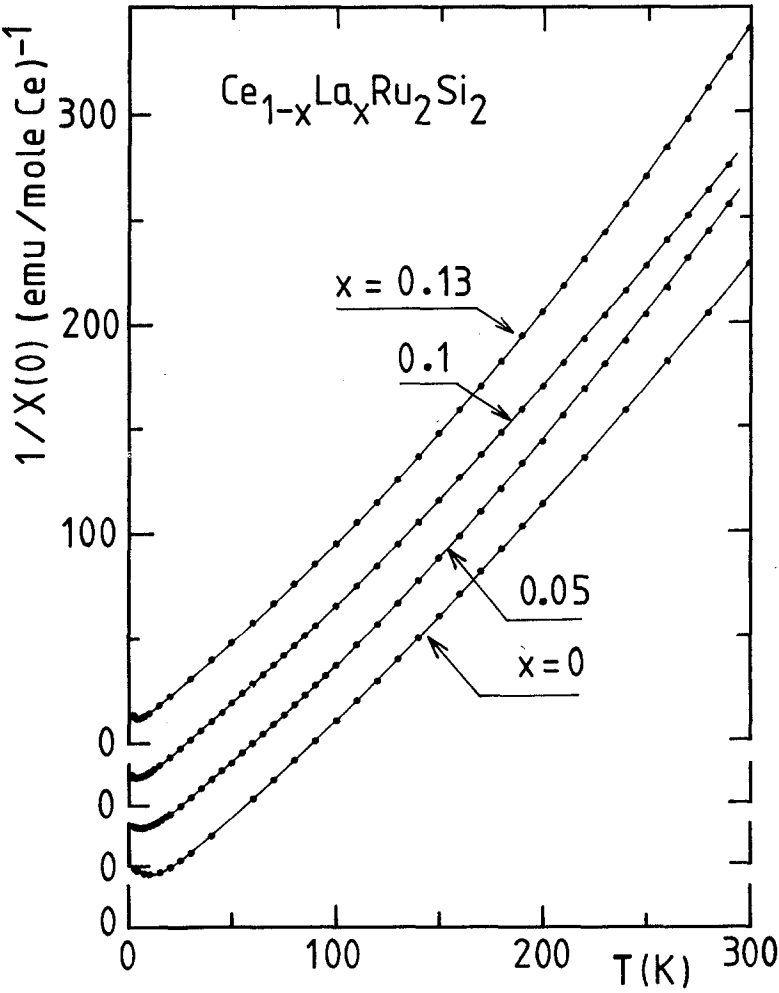

Fig. 1. Temperature variation of the inverse of the initial susceptibility, $1/\chi(0)$ [$=1/(\partial M/\partial H)_T$ at low field], from 1.5 to 300 K for single crystals of $Ce_{1-x}La_xRu_2Si_2$ with $x=0$, 0.05, 0.1, 0.13. The magnetic field was applied parallel to the tetragonal c axis.

upwards by 30 mole/emu. The χ^{-1} data cannot be fitted by an expression linear in temperature over any wide temperature interval. For $x=0$, if χ^{-1} is forced to obey the Curie–Weiss law, $\chi_c = D/(T+\theta)$, the value of θ is low but negative for $T \geq 120$ K, reaches zero for $T \sim 120$ K and is clearly positive below 70 K. This behavior is quite similar to that reported previously[1] for a small single crystal of $CeRu_2Si_2$, except that a linear behavior of χ^{-1} with $\theta \approx 0$ was observed above ~ 70 K almost to room temperature. Compared with the latter, the present data show a slight upturn of χ^{-1} for $T \geq 220$ K.

Specific-heat measurements have been analyzed with a doublet ground state and a first excited level at 220 K.[7] The ground state is mainly the $|\pm 5/2\rangle$ doublet which is highly anisotropic ($g_\parallel = 5g_J, g_\perp = 0$); the saturation moment is evaluated as $\sim 1.9\mu_B$.[7c,8] For such an anisotropic ground state, the Curie constant D of the Curie law ($\chi_c = D/T$) is higher along the c axis than that for the isotropic $J=5/2$ full angular momentum [$g_J^2\mu_B^2(J_z=5/2)^2/3k_B$ compared with $g_J^2\mu_B^2 J(J+1)/3k_B$]. The upturn of χ^{-1} for $T > 220$ K may result from the decrease of χ as the excited states are populated. Down to 70 K, it is difficult to extract any Kondo coupling from the susceptibility. Neutron measurements show that below 70 K local fluctuations and intersite fluctuations[4] have comparable magnitude. Furthermore, neutron measurements[16] indicate the simultaneous existence of ferromagnetic and antiferromagnetic fluctuations that, together with the large anisotropy, provide conditions favorable for the realization of metamagnetic properties. Thus, the susceptibility of $CeRu_2Si_2$ is certainly far from that of a single ion. It is also noteworthy that inelastic neutron experiments have failed to show any crystal-field splitting.[16,17] The possibility of observing the crystal-field splitting by specific heat and the difficulty of its detection dynamically is well known in heavy-fermion compounds when there is a strong competition between intersite and local coupling.[18]

As shown in Fig. 1, for the $Ce_{1-x}La_xRu_2Si_2$ alloys the high-temperature behavior of χ^{-1} is similar to that of $CeRu_2Si_2$. Figure 2 represents (on the same scale) χ^{-1} for the four systems below 80 K; strong departures between the different curves occur at low temperature. This figure and Fig. 1 also show that the deviation from a linear behavior with $\theta = 0$ occurs at lower temperature when the lanthanum content increases.

The low-temperature behavior of χ is represented in Fig. 3. The maximum of χ, at a temperature $T(\chi_{max})$ is broad for $x=0$ and 0.05 for which the ground state is a Pauli paramagnet; $T(\chi_{max})$ is shifted to lower values when La is substituted for Ce, from $\simeq 10$ K for $x=0$ to 6.5 K for $x=0.05$. The χ versus T curve of the alloy with $x=0.1$ is similar. It shows a maximum at $T(\chi_{max}) = 4$ K, which is not related to the occurrence of long-range order: we will see later that a value of the order of 2.9 K can be derived for T_N from magnetization measurements while the specific heat shows a small

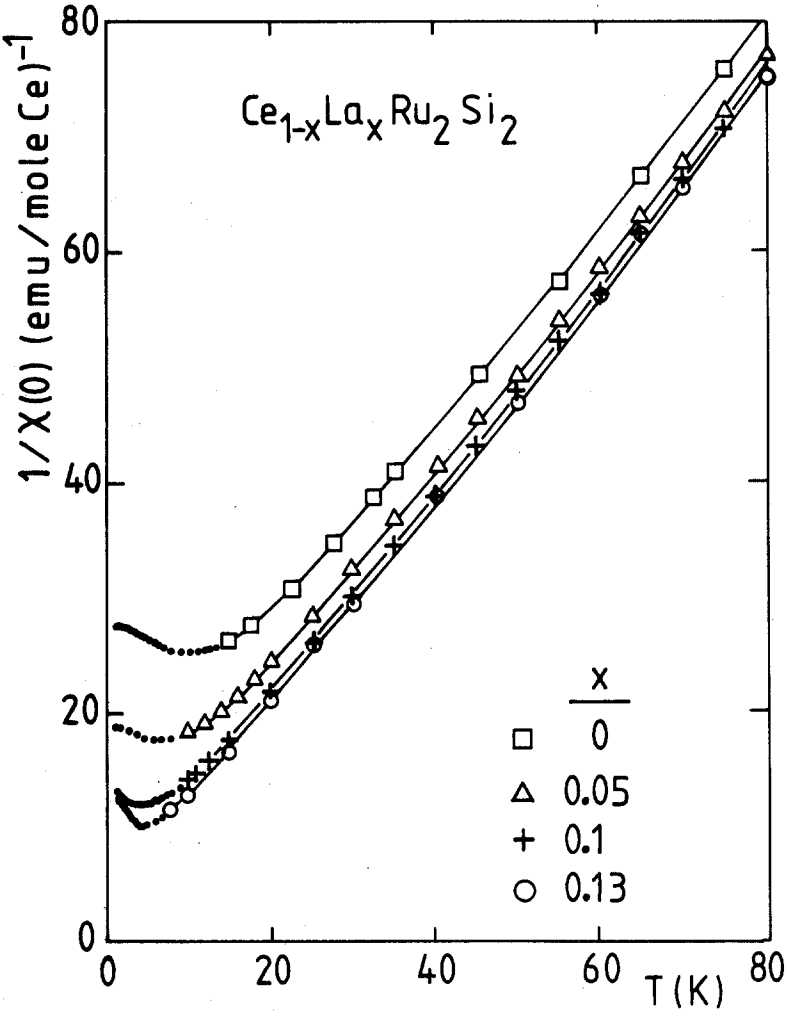

Fig 2. Expanded plot of the $T \leq 80$ K data from Fig. 1.

anomaly near 2.7 K. The Néel temperatures estimated by, respectively, neutron-diffraction experiments, $T_N(n)$[5]; by the location of the specific-heat anomaly $T_N(C)$; and by magnetization $T_N(M)$ are shown by different arrows (their different values will be discussed later). Increasing the amplitude of the moment modulation m_0 of the magnetic structure (from $0.8\mu_B$ for $x=0.1$ to $1.1\mu_B$ for $x=0.13$)[5] and the value of T_N leads to a sharp susceptibility maximum just above T_N, characteristic of long-range magnetic ordering as shown for $x=0.13$. Far below $T(\chi_{max})$, and below a characteristic

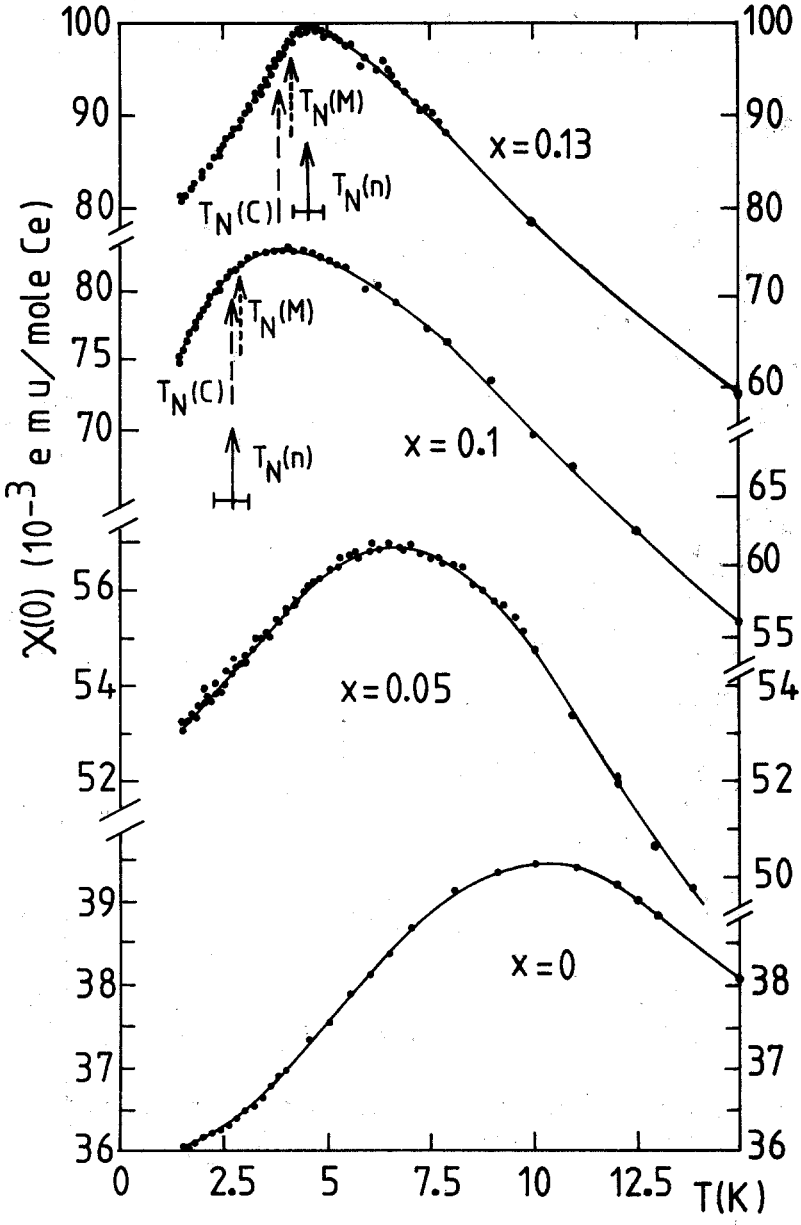

Fig. 3. Temperature dependence of the initial susceptibility at low temperatures.

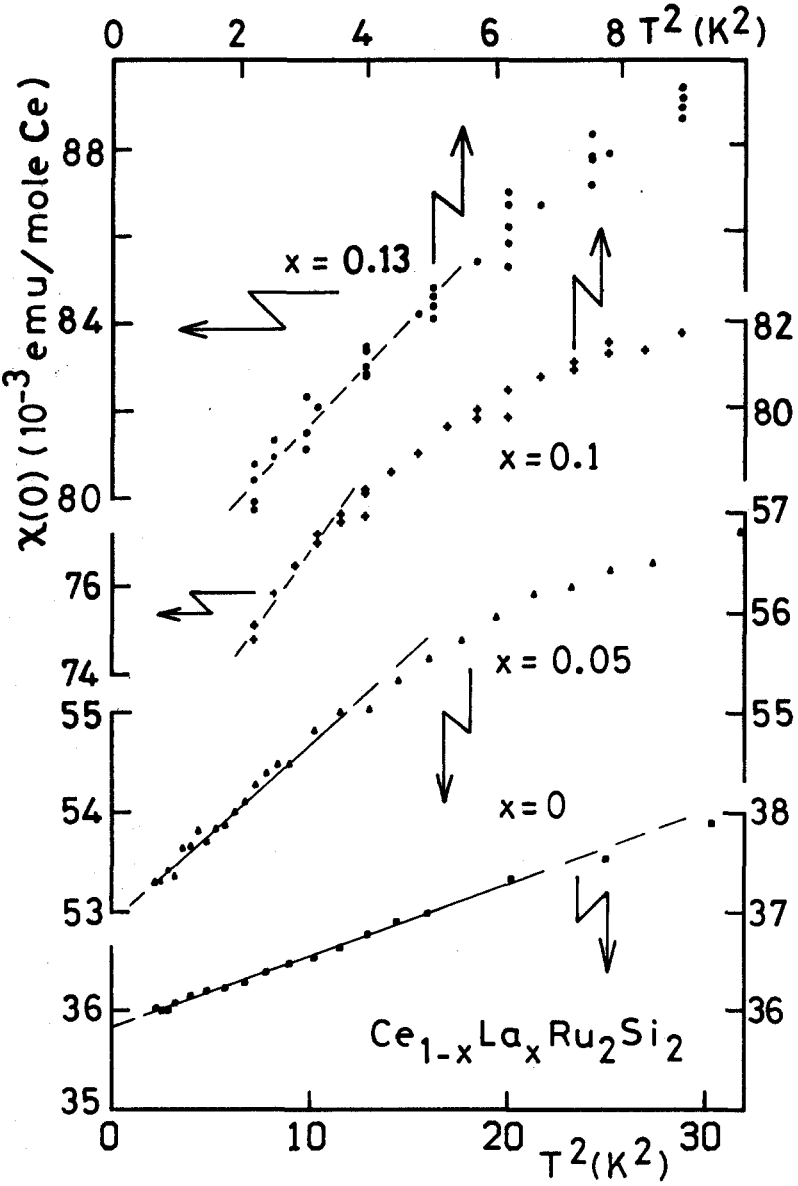

Fig. 4. Plots of $\chi(0)$ versus T^2 for $x=0$ and 0.05 (lower T^2 scale) and for $x=0.1$ and 0.13 (upper T^2 scale).

TABLE I
Parameters of the $Ce_{1-x}La_xRu_2Si_2$ Compounds at $H=0$*

x	χ_0 (emu mole^{-1})	A (emu mole^{-1} K^{-2})	T^* (K)	$(A/\chi_0^2)_{norm}$	$(\gamma/\chi_0)_{norm}$	$\gamma_{T\to 0}$ (mJ mole^{-1} K^{-2})
0	0.0358	7.16×10^{-5}	4.5	1	1	360
0.05	0.0528	1.72×10^{-4}	3.4	1.10	1	530
0.1	0.070 ± 0.001	$(1.85\text{–}2.25)\times10^{-3}$	1.8 ± 0.1	6.8–8.2	0.92	650
0.13	0.076 ± 0.001	$(1.54\text{–}2.27)\times10^{-3}$	1.7–3	4.7–7.2	~0.5	~390

*χ_0 and γ are the extrapolation of $\chi(H\to0)$ and C/T $(H=0)$ at $T\to0$. Mole refers to 1 nmole Ce. T^* is the temperature below which the susceptibility can be described just by an additional quadratic AT^2 term.

temperature T^*, the susceptibility of the two PP compounds has a quadratic temperature dependence $\chi=\chi_0+AT^2$ (see Fig. 4) as expected for such systems. Also shown in Fig. 4 are plots of χ *versus* T^2 for $x=0.1$ and 0.13, which also show a linear variation below $T^*(<T_N)$. The values of χ_0, A, T^*, and the ratio A/χ_0^2 (the latter normalized to the $x=0$ case) are given in Table I. Clearly, a change occurs between PP and AF compounds. If χ_0 is proportional to the inverse of a characteristic temperature T_{sf}, and the problem reduced to a unique variable, A/χ_0^2 should be a constant. Although it cannot be determined precisely for $x=0.1$ and 0.13, this ratio appears to be much larger in these two cases than for $x=0$ and 0.05.

3.2. High-Field Magnetization and Differential Susceptibility

The magnetization curves in high magnetic fields at 4.2 and 1.4 K are shown respectively in Figs. 5 and 6. An inflection point in $M(H)$ appears at 4.2 K (i.e., in the PP state) for all of the compounds at a characteristic field H_M. For the nonmagnetically ordered alloy $Ce_{0.95}La_{0.05}Ru_2Si_2$, this inflection can be seen up to ~15 K as shown by the plot of $\chi(H)$ in Fig. 7. For $x=0.13$, a magnetically ordered alloy, two steps occur in $M(H)$ at 1.4 K (i.e.. below T_N), at fields H_a (of the order of 1 T) and H_c (of the order of H_M). For the other ordered alloy, $x=0.1$, the existence of similar steps in the 1.4 K $M(H)$ curve is not obvious. Characteristic effects are better seen on analyzing the plots of $\chi(H)$ of Figs. 8 and 9. For both magnetically ordered alloys, peaks (at H_a and H_c) start to grow, while a broad maximum in $\chi(H)$ persists at $H_M>H_c$ over a large temperature range. H_M seems to reach H_c only at very low temperature, notably, for $x=0.1$; The location of H_a, H_c, and H_M are shown in Fig. 10 as $H-T$ phase diagrams. For $x=0$, 0.05, and 0.1, it must be noticed that H_M shows a maximum at a temperature almost identical to the temperature $T(\chi_{max})$ of the maximum of $\chi(T)$ observed in zero field (Fig. 3).

If the value of $T_N(M)$ is defined as the temperature where the first peak (at H_a) emerges, $T_N(M)$ is equal to 2.9 and 4.1 K for $x=0.1$ and 0.13,

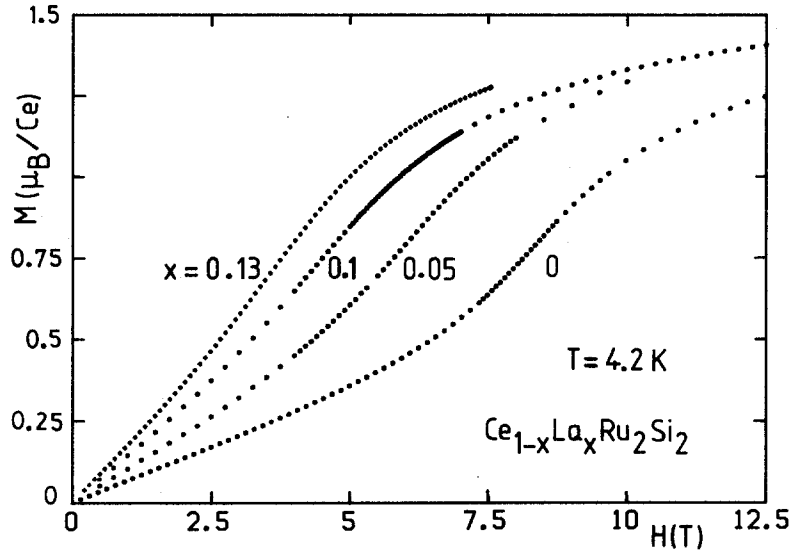

Fig. 5. Magnetization at $T=4.2$ K as a function of the magnetic field for $x=0$, 0.05, 0.1, 0.13.

respectively. This appears to be the most reliable determination of T_N: The difficulty of observing magnetic order for $x=0.1$ by other macroscopic techniques is obvious (the absence of an anomaly in $\chi(0)$; a very small anomaly in C; previous C measurements[7] on polycrystalline samples failed to reveal this order). It seems worthwhile to emphasize that for $x=0.13$, where all the measurements were made on the same crystal, the differences in the values of T_N derived from different determinations (Fig. 3) are not attributable to any temperature or La concentration uncertainty but rather have some physical meaning. The value $T_N(n)$, derived from neutron experiments, is affected by an error bar that results from the fact that the temperature dependence of the magnetic Bragg intensity shows a tail and not an abrupt decrease to zero.[5] The value $T_N(M) \sim 4.1$ K lies within this error bar. (Notice that, as is usual, it is lower than the temperature (4.6 K) of the maximum of $\chi(0)$ (Fig. 3). It would correspond to an inflection point in the $\chi(0)$-T curve but that cannot be determined within the precision of the data.) In this case the temperature of the maximum in C at 3.8 K is noticeably lower than $T_N(M)$, but for higher La concentrations, the temperature of the specific-heat peak becomes closer to that of the inflection point in the susceptibility (see curve in Ref. 8b).

Plots of χ versus H at 4.2 K, where all the compounds are PP, are shown in Fig. 11. The maximum $\chi(H_M)$ is sharper for $x=0$ than for the lanthanum-doped compounds. This difference becomes more pronounced

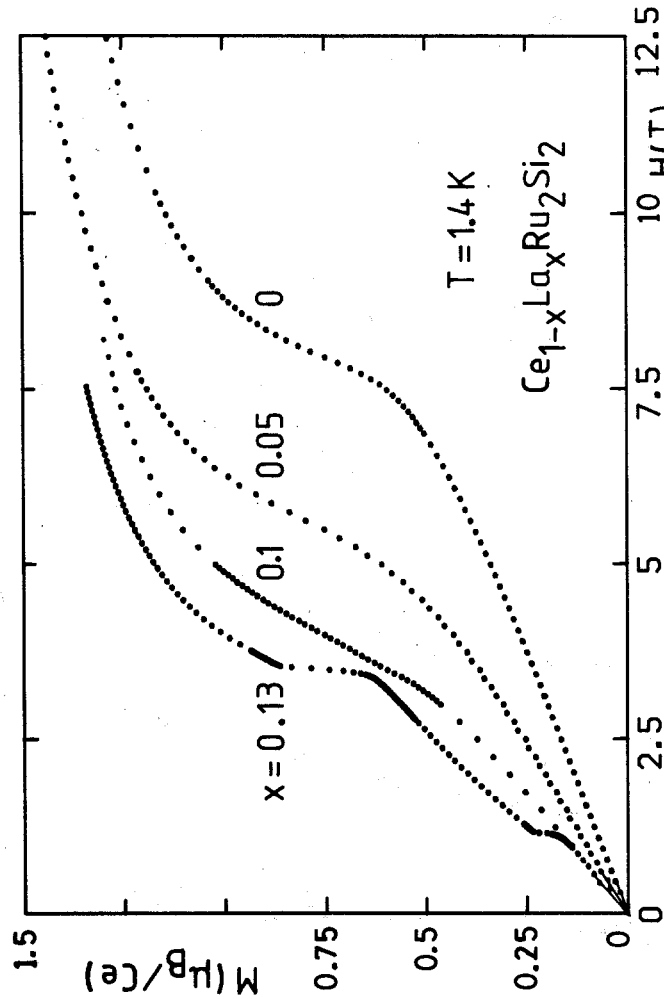

Fig. 6. Magnetization at $T = 1.4$ K as a function of the magnetic field for $x = 0$, 0.05, 0.1, 0.13.

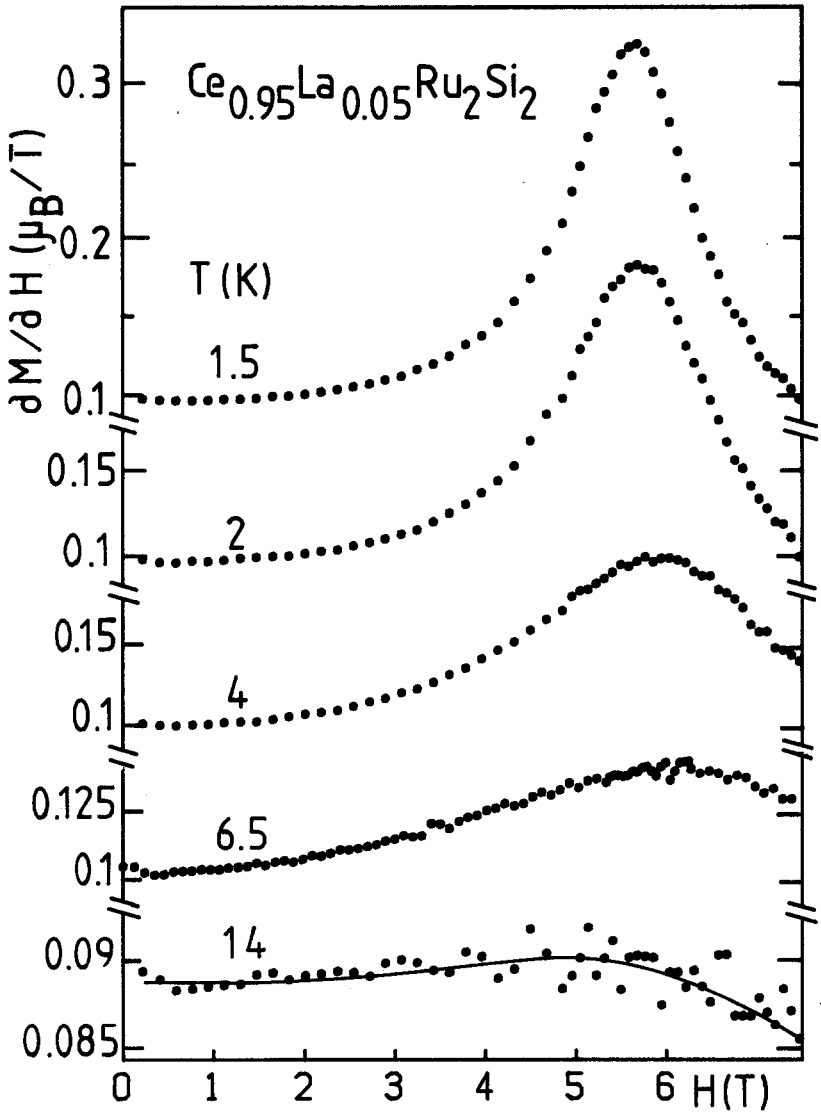

Fig. 7. Field variation of the differential susceptibility $\chi(H)$ $[=(\partial M/\partial H)_T]$ at different temperatures for $x=0.05$.

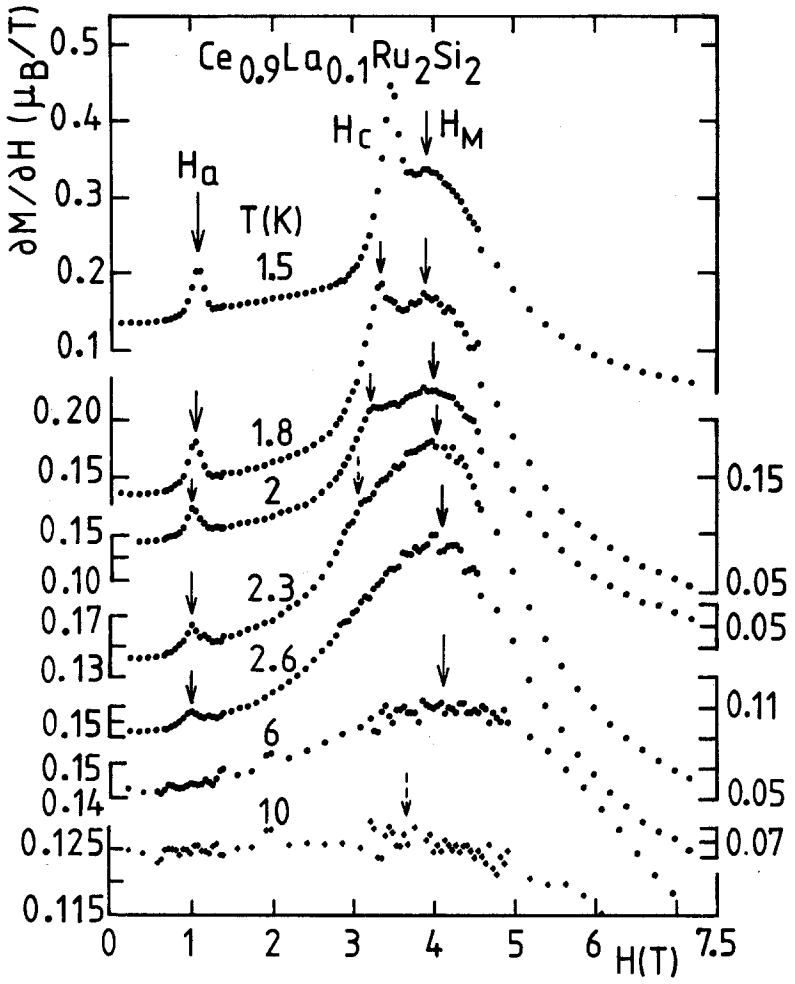

Fig. 8. Field variation of the differential susceptibility $\chi(H)$ $[=(\partial M/\partial H)_T]$ at different temperatures for $x=0.1$. Arrows show the characteristic fields H_a, H_c, and H_M.

on cooling; there is also a large increase of $\chi(H_M)$ for the PP systems $x=0$ and $x=0.05$ as shown by the plots of Fig. 12. Defining a width ΔH_M of the magnetic transition by the width of the $\chi(H)$ peak at half height, i.e., at $\chi(0)+[\chi(H_M)-\chi(0)]/2$ leads at 1.4 K to ΔH_M equal to 0.43 and 0.68 T, respectively, for $x=0$ and $x=0.5$. Clearly, for PP ground states, the metamagnetic anomalies are sharper for the pure lattice. Furthermore, $\chi(H_M)$ increases strongly on cooling. The rounding of $\chi(H)$ at $H\to H_M$ is not produced by effects of a large demagnetization field H_D. For $x=0$, $H_D\approx 0.034T$

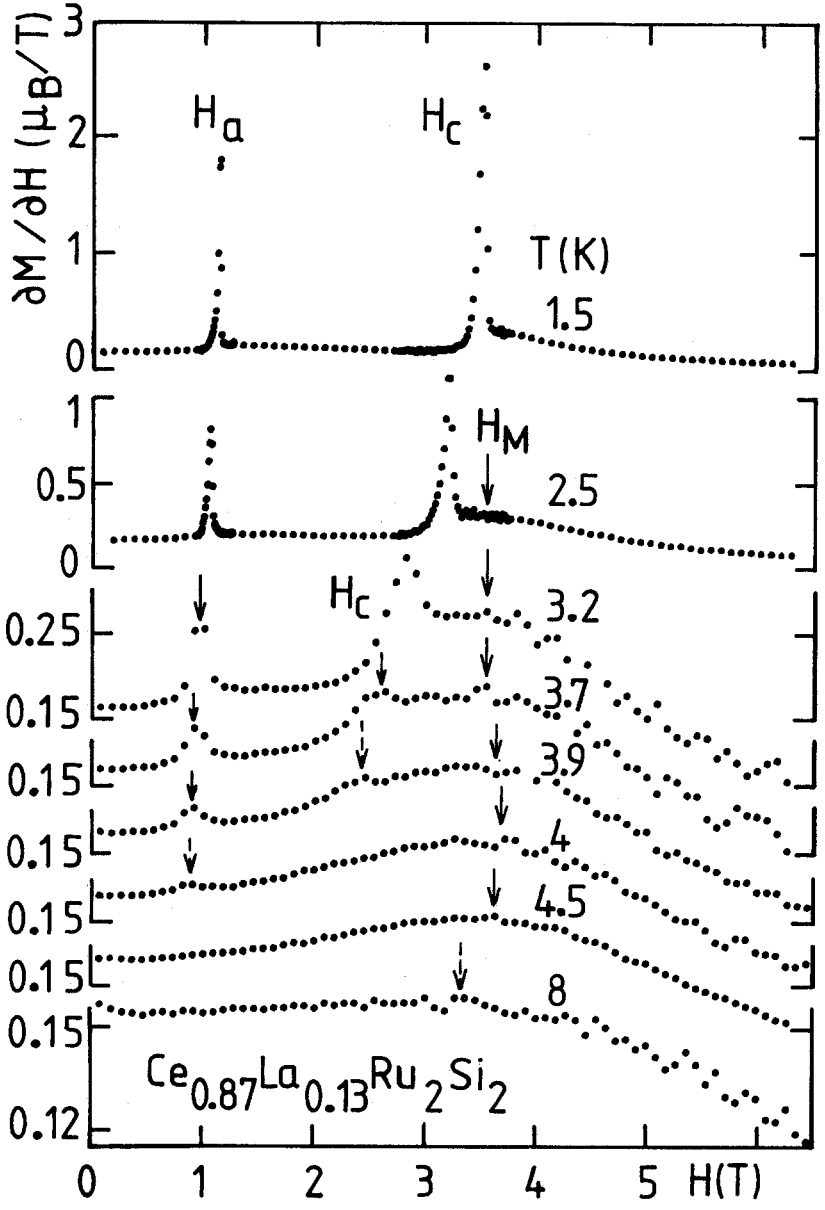

Fig. 9. Field variation of the differential susceptibility $\chi(H)$ $[=(\partial M/\partial H)_T]$ at different temperatures for $x=0.13$.

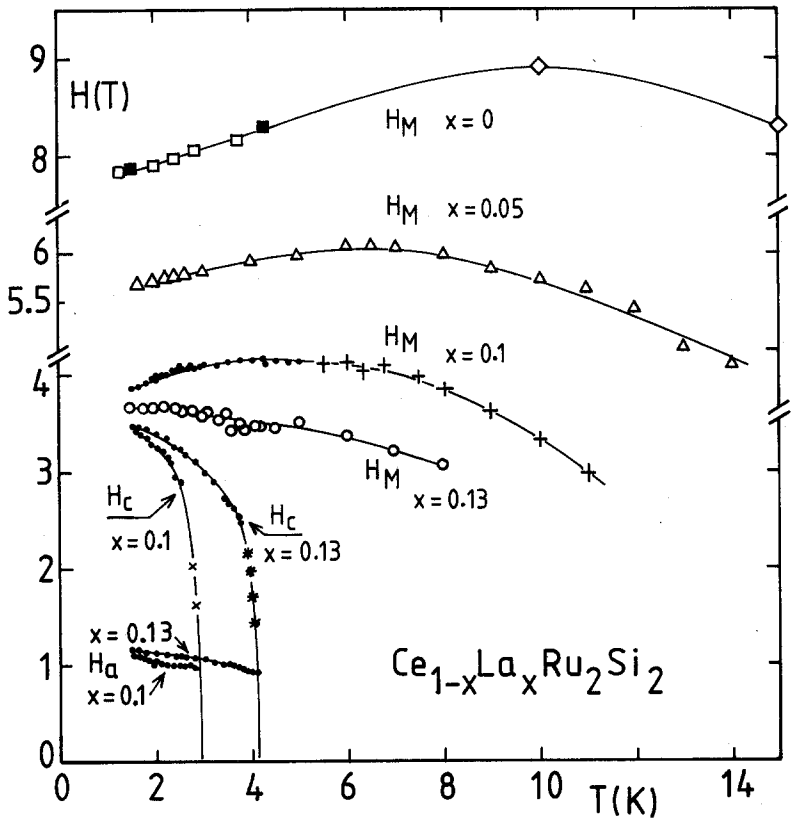

Fig. 10. $H-T$ phase diagram. Location of H_a, H_c, and H_M as defined in the text. For $x=0$: (■) present data; (□) Ref. 28; (◇) from Ref. 1. The data points labeled × ($x=0.1$) and ∗ ($x=0.13$) were determined from M versus T measurements at constant H.

at $H_M \sim 8$ T and $T \sim 1.4$ K (disc of 4 mm radius by 2 mm thickness). If an attempt is made to represent $\chi(H_M)$ by a Curie–Weiss law, measurements on different samples of $CeRu_2Si_2$ give values of θ ranging between 0.1 and 1 K. Furthermore, θ increases with x, reaching, for example, 3 K for $x=0.13$.

4. SPECIFIC HEAT. COMPARISON BETWEEN DIFFERENT ALLOYS

4.1. $H=0$

The specific heats of the different samples, after subtraction of the specific heat of $LaRu_2Si_2$, which was taken from the data of Ref. 7 ($\gamma=$

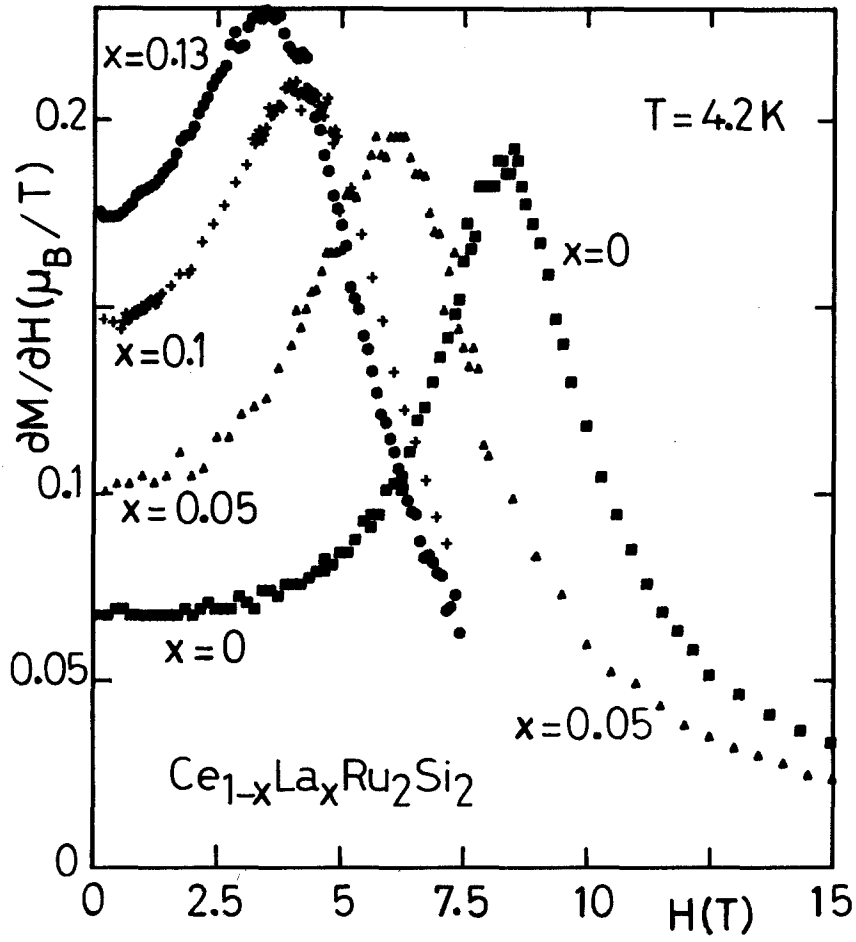

Fig. 11. $\chi(H)$ $[=(\partial M/\partial H)_T]$ at 4.2 K for $x=0$, 0.05, 0., and 0.13.

6.5 mJ mole^{-1} K^{-2}, $\theta_D=320$ K), are shown in Fig. 13. A peak in C at $T_N(C)\sim 3.8$ K for $x=0.13$ corresponds to the AF ordering, and a small plateau occurs just above this peak. For the other AF ordered sample with $x=0.1$, the signature of magnetic ordering is given only by a shoulder centered near $T_N(C)=2.7$ K. For the PP ground state cases ($x=0$ and $x=0.05$), qualitatively the specific heat has a behavior similar to that predicted by Kondo models. However, quantitative differences appear. For example, for $x=0$, the maximum of $C=2.25$ J mole^{-1} K^{-1} at $T(C_{max})\sim 11.3$ K is higher than the universal value $C=1.45$ J mole^{-1} K^{-1} predicted for a single Kondo ion for an $S=1/2$ doublet ground state.[7] The extrapolated values of

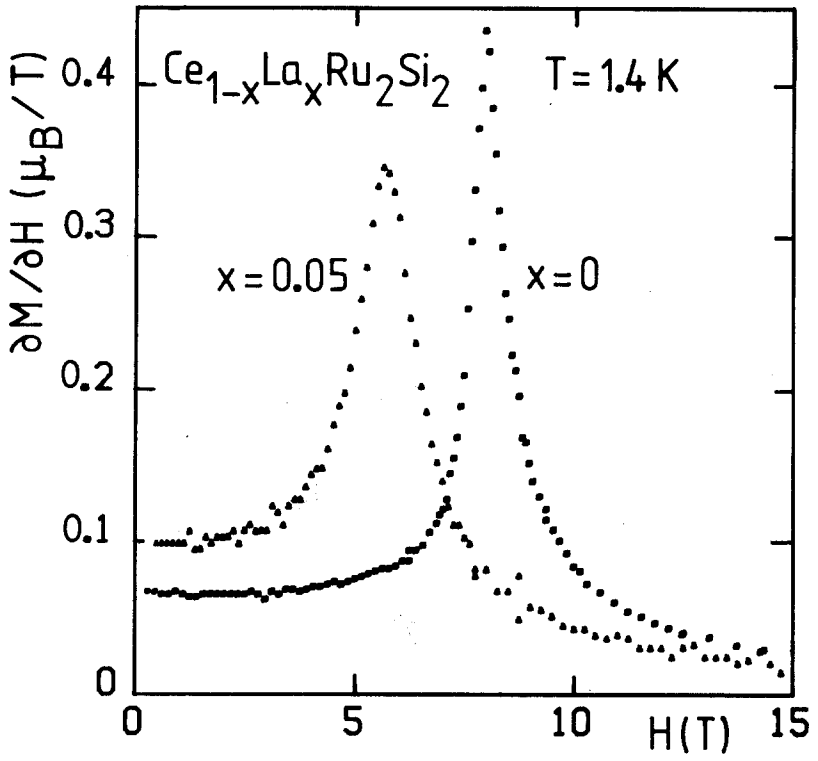

Fig. 12. $\chi(H)$ $[=(\partial M/\partial H)_T]$ at 1.4 K for the PP cases ($x=0$ and 0.05).

$\gamma \equiv (C/T)_{T\to 0}$ are 360 mJ mole^{-1} K^{-2} and 530 mJ mole^{-1} K^{-2} for $x=0$ and $x=0.05$, respectively (Fig. 14). The products $\gamma TC_{\max}$) are, respectively, 4090 and 3950 mJ mole^{-1} K^{-1}. If $T(C_{\max})$ is used to estimate an effective Kondo temperature through the usual relation $T(C_{\max})=2.2T_K$, one gets $T_K=25$, 16.4, and 12.5 K for $x=0$, 0.05, and 0.1, respectively. The ratios γ/χ_0 normalized to $x=0$ (given in Table I) are almost identical for $x=0$, 0.05, and 0.1. For $x=0.13$, C/T remains high ($\sim$645 mJ mole^{-1} K^{-2}) below 3.5 K, until a kink in C/T occurs at $T=0.6$ K i.e., far below $T_N(C)$. A linear extrapolation of C/T below this kink leads to a low value of γ, $\sim$390 mJ mole^{-1} K^{-2}, and consequently a drastic decrease of the γ/χ_0 ratio. A drop of γ/χ_0 has been observed at T_N in the archetypical Kondo AF $CeAl_2$.[19] It is also worth mention that here in the AF systems ($x=0.1$ and 0.13) inflection points occur in the temperature variation of C/T near T_N. By contrast, for $x=0$ and $x=0.05$, C/T varies quasilinearly with T. Such a variation has been observed for the archetypical PP heavy-fermion compound $CeCu_6$.[13,20]

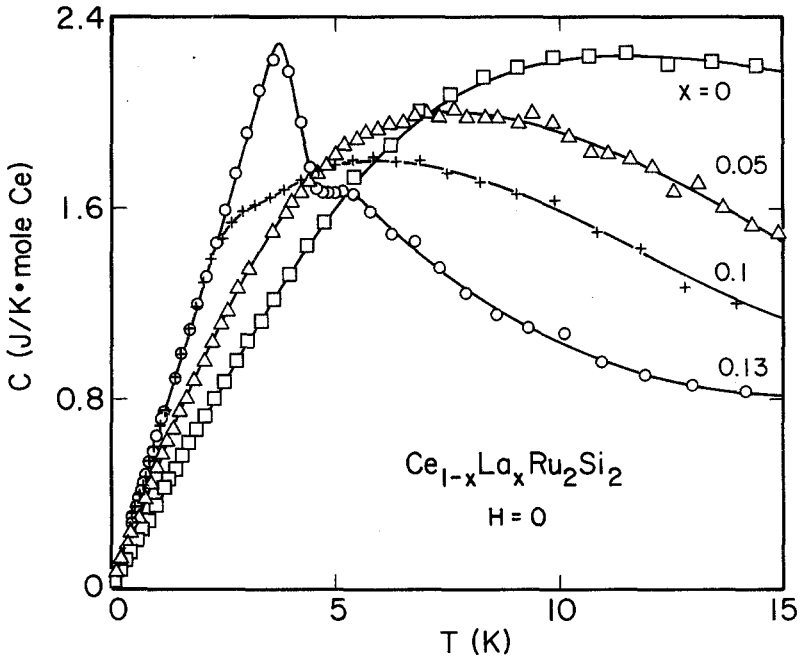

Fig. 13. Specific heat versus temperature for the $Ce_{1-x}La_xRu_2Si_2$ alloys at $H=0$, after subtraction of the specific heat of $LaRu_2Si_2$ (taken from Ref. 7).

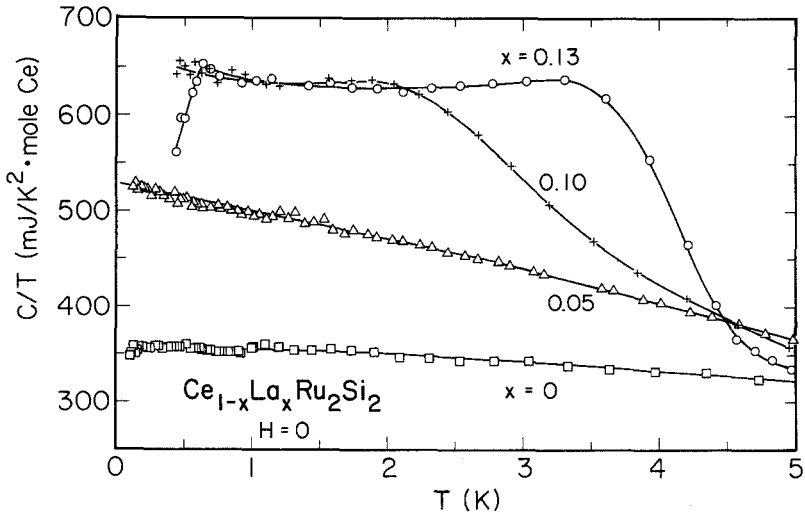

Fig. 14. Data of Fig. 13 replotted as C/T versus T.

The specific-heat data for $CeRu_2Si_2$ reported here differ from the results of some earlier measurements. In the plot of C/T versus T in Ref. 7a (where C is, as here, the specific heat of $CeRu_2Si_2$ corrected by subtraction of that of $LaRu_2Si_2$), a weak maximum appears near 4 K. The extrapolation to $T=0$ leads to a value of 320 mJ mole^{-1} K^{-2}, notably lower than our result. In the data reported in Ref. 13, a very weak maximum of C/T might also occur above 1 K; here a value of 350 mJ mole^{-1} K^{-2} can be obtained by extrapolation to $T=0$, in better agreement with our result. (However, it seems that the specific heat of $LaRu_2Si_2$ is not subtracted in the data of Ref. 13; making this correction leads to $(C/T)_{T\to 0}\sim 343$ mJ mole^{-1} K^{-2}). The other values reported for polycrystals are higher than ours: from Ref. 14, one deduces after subtracting C of $LaRu_2Si_2$, $(C/T)_{T\to 0}\sim$ 380 mJ mole^{-1} K^{-2}, while in Ref. 15 a value of $\sim$375 mJ mole^{-1} K^{-2} at 1.5 K is reported. The discrepancies between these different measurements are too large to be attributed to the fact that they are not taken at the same temperature, or were differently extrapolated to $T=0$ (our data lead to $C/T=350$ mJ mole^{-1} K^{-2} at 1.5 K compared with 360 mJ mole^{-1} K^{-2} at $T=0$). These discrepancies might also depend on the purity of the starting materials: when given, the latter is about 4N, except for Ref. 14, where the Ru is only 3N. Another possibility is that polycrystalline samples contain parasitic phases (of the order of a few percent, i.e., not detectable by x-ray analysis) which do not have the same specific heat as the pure phase. This can also explain the observation of a very weak maximum in C/T above 1 K. We will see later that clear maxima in C/T occur for our crystal on applying a magnetic field.

The entropy, shown in Fig. 15, seems to confirm the existence of a well isolated crystal-field doublet. As usual, in AF Kondo lattices, the full entropy of the doublet $R\ln 2$ is recovered far above T_N. For $x=0$, 0.05, and 0.1, arrows show the position of $T(\chi_{max})$, the temperature of the maxima of $\chi(0)$. For the PP ground states, there is also a characteristic temperature $T(\alpha_{max})$ close to $T(\chi_{max})$] corresponding to the extremum of the thermal expansion (α) (see Refs. 9 and 21). At $T(\alpha_{max})$ or $T(\chi_{max})$ ($H=0$), the entropy has roughly the value of that found at T_N for AF alloys. The thermal expansion is a derivative technic directly related via the Maxwell equation to the pressure derivative of the entropy. Since it is huge here due to the proximity of a magnetic instability, $T(\alpha_{max})$ is well defined. We will use in the discussion the field dependence of T (α_{max}) as a characteristic crossover temperature. For $T<T(\alpha_{max})$, magnetism and electronic motion are strongly coupled.[21] $T(\alpha_{max})$ may be directly connected to the temperature T^* below which the Fermi liquid properties are observed.

4.2. $H\sim H_M-\varepsilon$

The specific heat for $H\sim H_M-\varepsilon$ or $H_c-\varepsilon$, i.e., just below H_M for $x=0$ and 0.05, and just below H_c for $x=0.1$ and 0.13 is plotted in Fig. 16. A

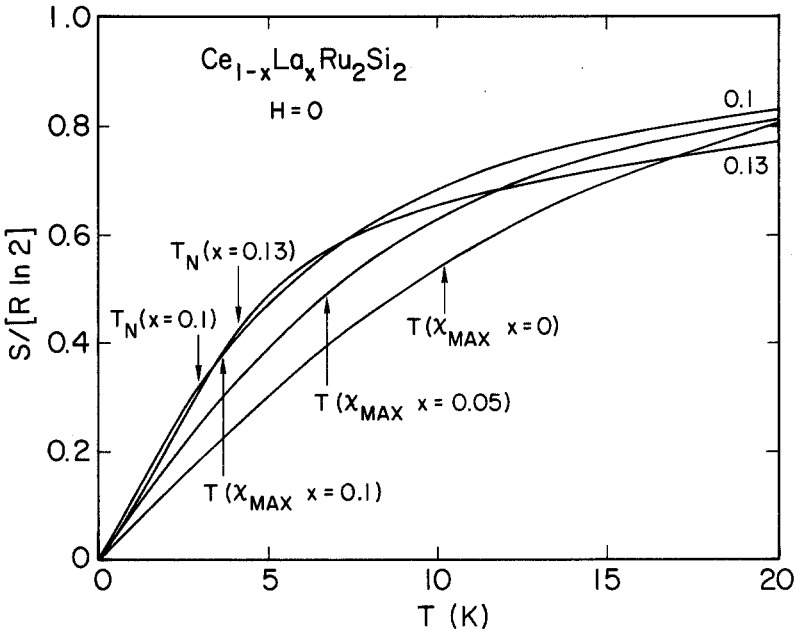

Fig. 15. Entropy versus T at $H=0$. The arrows are defined in the text.

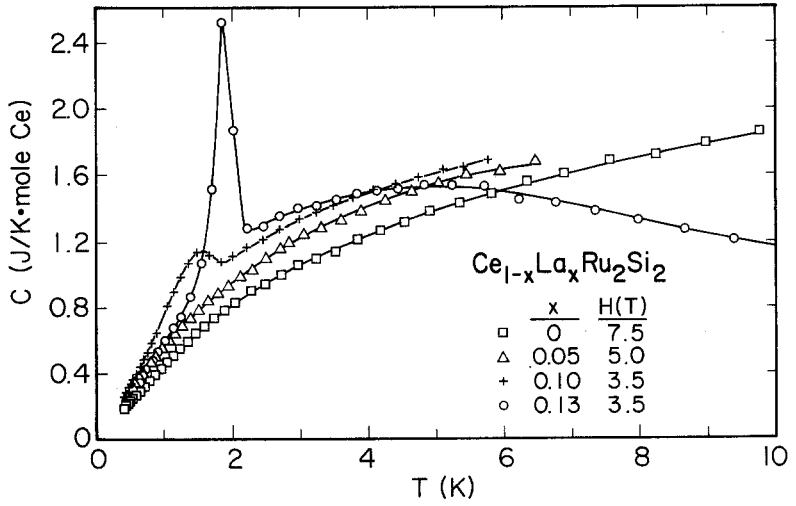

Fig. 16. Specific heat at $H \sim H_M - \varepsilon$ ($x=0$ and 0.05) or $H \sim H_c - \varepsilon$ ($x=0.1$ and 0.13).

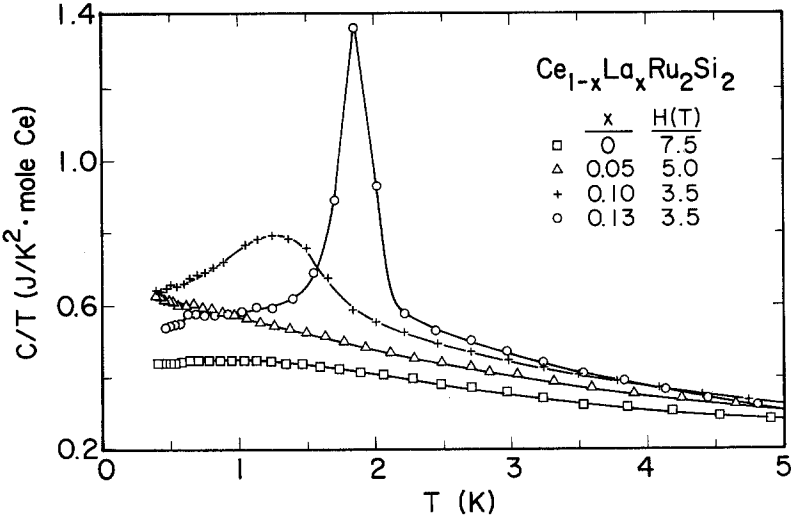

Fig. 17. Data of Fig. 6 for $T \leq 5$ K, replotted as C/T versus T.

specific-heat anomaly at $T_N(H_c)$ is clearly displayed for the two AF alloys. Furthermore, these anomalies are now sharper than at $H=0$. By contrast, no peak occurs for the PP cases. However, the temperature dependence of C/T reveals the existence of a maximum for $x=0$ and a continuous increase of C/T is still observed for $x=0.05$ in the vicinity of H_M (Fig. 17).

4.3. $H \gg H_M$ or H_c

Applying a magnetic field larger than H_M or H_c leads to similar C and C/T curves (Figs. 18 and 19) for $x=0.05$, 0.1, and 0.13. The temperature of the maxima in C/T increases with H. This behavior is qualitatively characteristic of a Zeeman decoupling between spin-up and spin-down bands.[15]

5. SPECIFIC HEAT ANALYSIS AT CONSTANT x

5.1. $x=0$

Figures 20 and 21 represent the variation of C/T versus T for the pure Ce Ru_2Si_2 compound for different applied fields. For $H_M > H \geq 5$ T (i.e., on approaching H_M), a maximum in C/T is clearly seen at a temperature $T([C/T]_{max})$ that decreases with increasing H: For $H=7.5$ T, it occurs near 0.8 K. It may be expected that for $H > H_M$, $T([C/T]_{max})$ will increase significantly with H, as observed on a polycrystalline sample for $H=12$ T.[15] For $H < H_M$, the variations of $T([C/T]_{max})$ as a function of H may mimic a phase-diagram

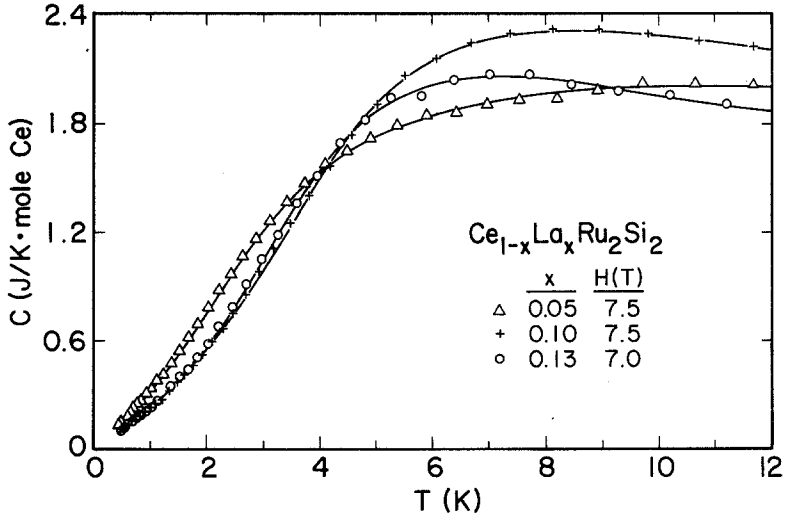

Fig. 18. Specific heat data for $H > H_M$ (as limited by available magnetic fields).

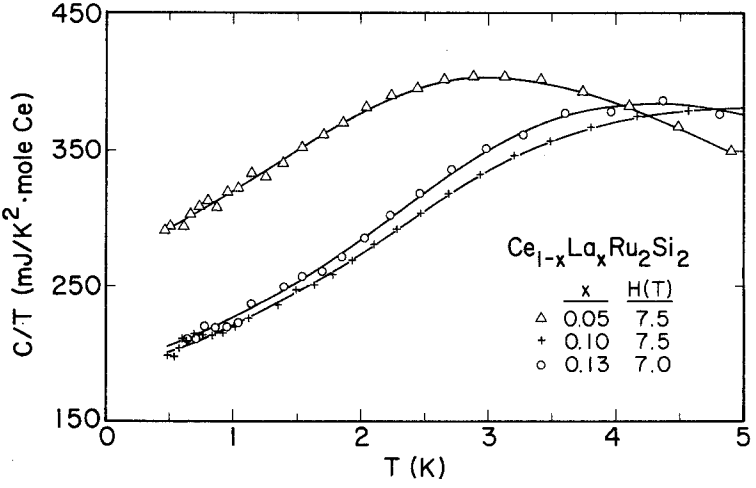

Fig. 19. Data of Fig. 18 for $T \leq 5$ K, replotted as C/T versus T.

boundary inside which the intersite correlations are strong. This phase diagram is far more difficult to draw than $[T(\alpha_{max}), H]$ previously mentioned.[9]

5.2. $x = 0.05$

By contrast with the behavior at $x = 0$, no maximum in C/T is observed for $x = 0.05$ for $H < H_M$ (Fig. 22a), but a strong field variation of C/T occurs

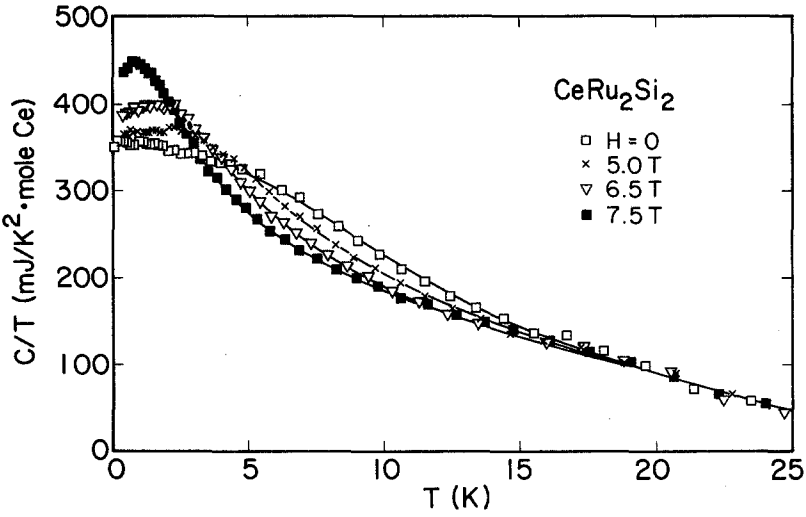

Fig. 20. C/T versus T for $x=0$, $T>25$ K and different magnetic fields.

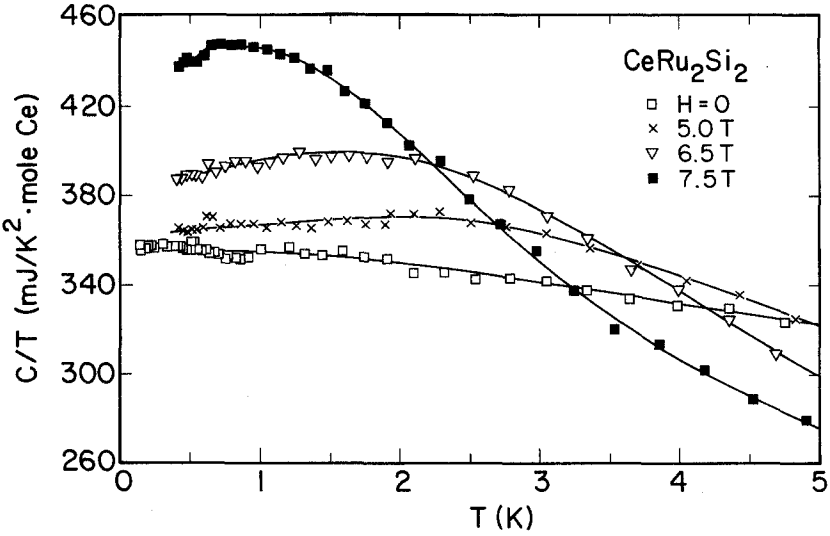

Fig. 21. Expanded plot of the $T<5$ K data of Fig. 20.

in the vicinity of H_M (~ 5.5 T) (Fig. 22b). A linear extrapolation of C/T versus T leads to an enhancement of γ at H_M of about 28% by comparison with the zero-field value, but it is obvious that the extrapolation of $\gamma(H)$ is

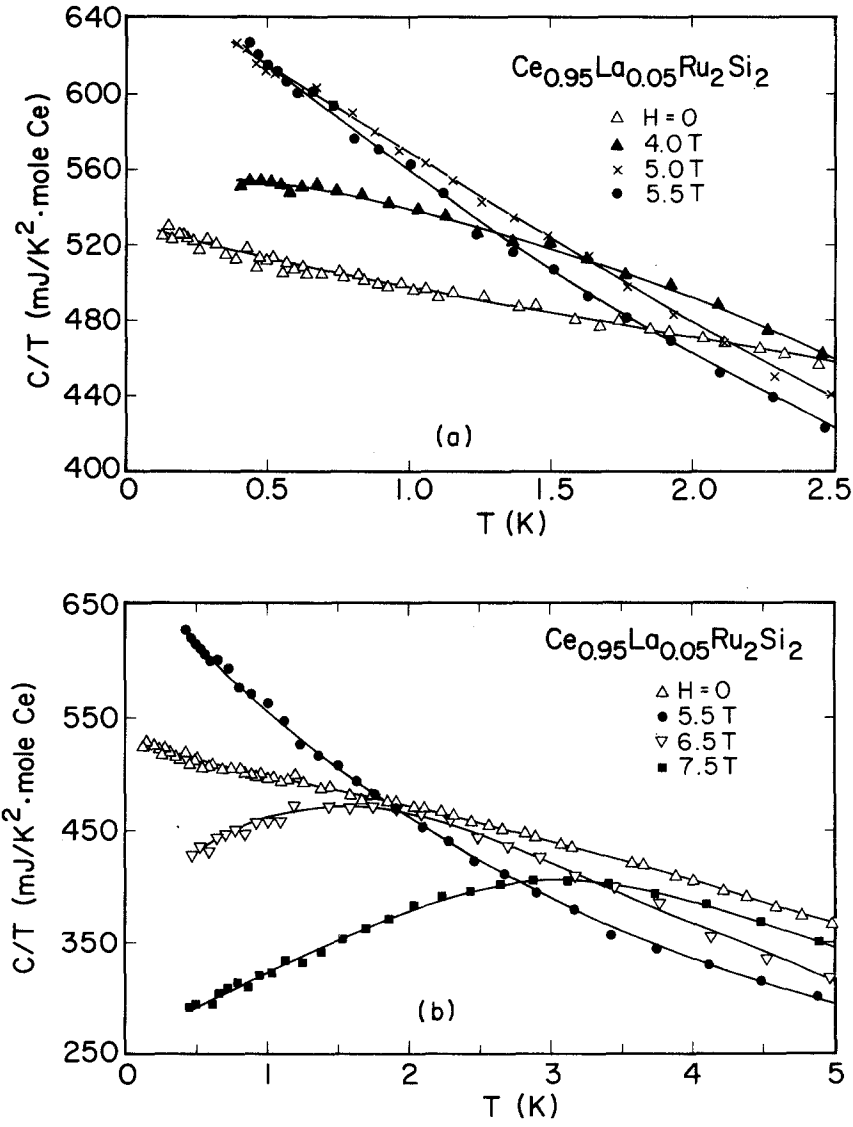

Fig. 22. C/T versus T for $x=0.05$, at different magnetic fields; (a) for $T \leq 2.5$ K; (b) for $T \leq 5$ K.

not unambiguous. Above H_M, a maximum in C/T appears and its position increases with H (Fig. 22b).

5.3. $x = 0.1$

As previously emphasized, the interesting feature for this concentration on the magnetic side of the magnetic-nonmagnetic transition is that the specific-heat anomaly at $T_N(H)$ becomes sharper in fields 2.5–3.5 T than for $H=0$ (Figs. 23–25). The ordinates of these peaks are consistent with the H_c-T phase diagram of Fig. 10 deduced from the magnetization measurements: on increasing H, the temperature of the maximum in C/T decreases; the value of H_c for $T\to 0$, $H_c(0)$, can be estimated as slightly higher than 4 T, since for this field C/T still shows a small anomaly near 0.8 K. Above $H_c(0)$, both C and C/T show rounded maxima at temperatures T_{max}, which

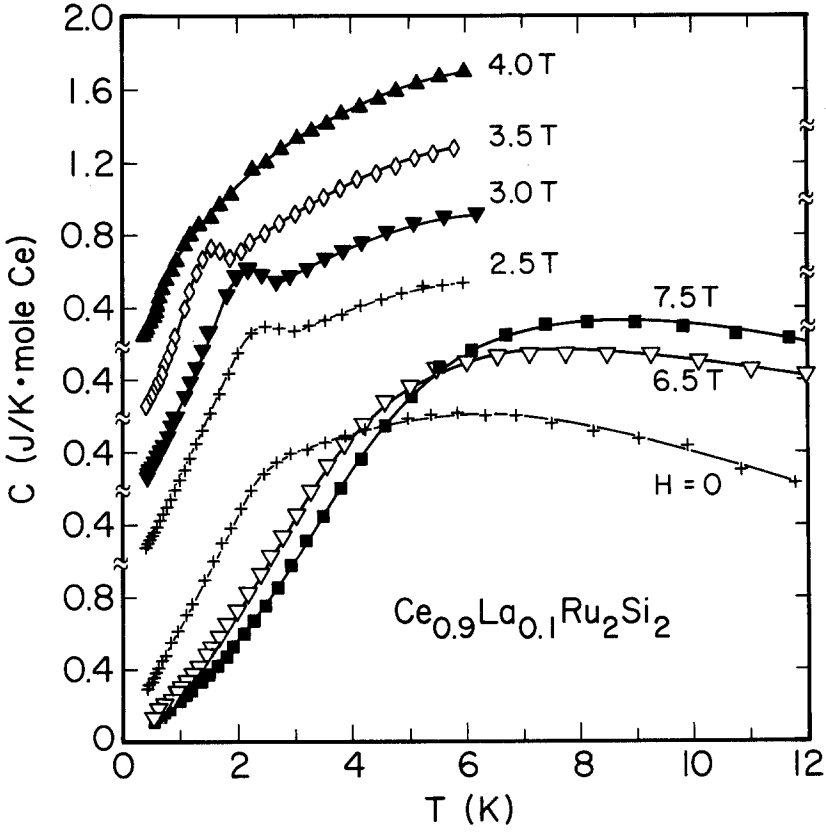

Fig. 23. C versus T for $x=0.1$, $T\leq 12$ K and different magnetic fields.

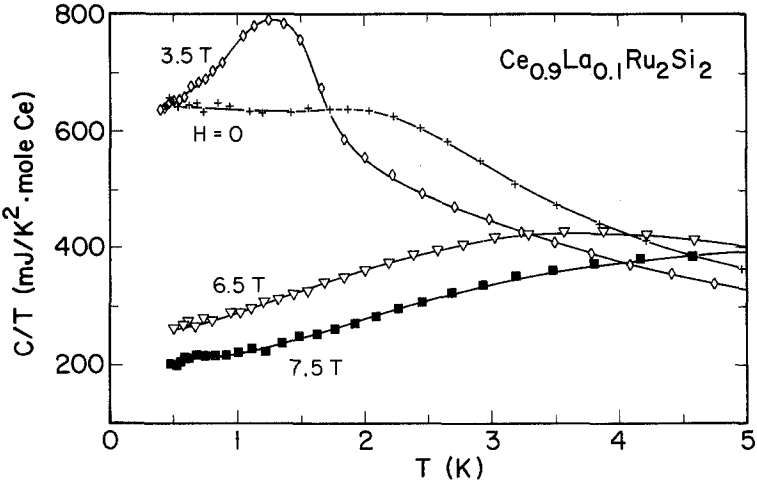

Fig. 24. Replot of some of the $T \leq 5$ K data of Fig. 23 as C/T versus T.

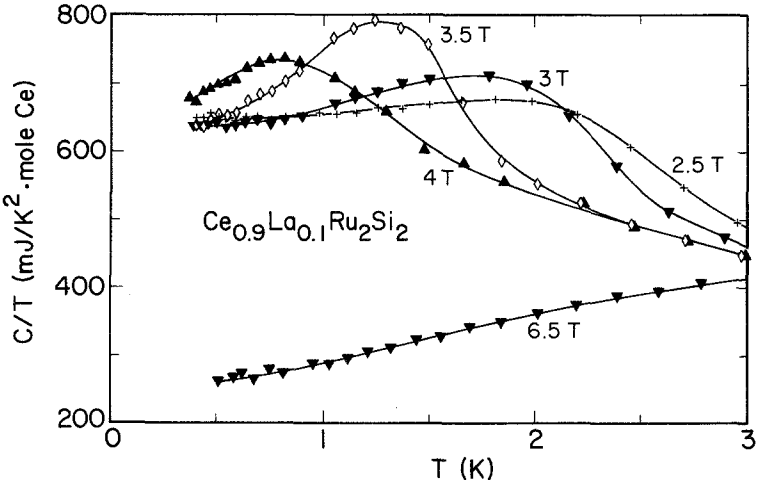

Fig. 25. Replot of some of the $T \leq 3$ K data of Fig. 23 as C/T versus T.

increases with H (Figs. 23 and 24). As previously emphasized, this feature is the same for all four systems.

5.4. $x = 0.13$

The data for the AF case, $x = 0.13$, are shown in Figs. 26 and 27. The considerations are analogous to those already made for $x = 0.1$. However,

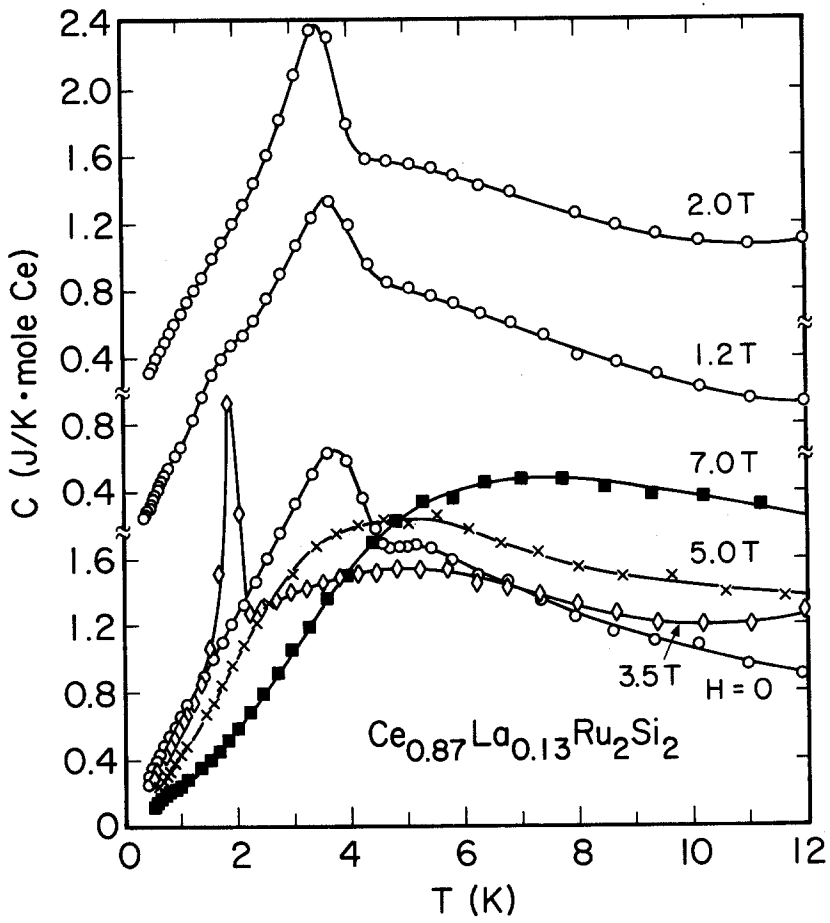

Fig. 26. C versus T for $x=0.13$, $T\leq 12$ K and different magnetic fields.

new features are observed for $H<H_c$, particularly visible in the C/T plots of Fig. 27. In addition to the peak occurring at $T_N(H)$, i) all curves for $H\leq 3.5$ T, exhibit a kink at a temperature close to 0.6 K, and ii) for $H=$ 1.2 T, a third specific-heat anomaly occurs at ~ 1.55 K. The temperature and field values of these different peaks are reported on the detailed low-temperature phase diagram of Fig. 28. Except for lower values of T_N, as discussed before, they are in good agreement with the phase diagram derived from magnetization measurements. The low-temperature dashed lines in this diagram were drawn by analogy with the rather complex phase diagram recently reported for a $Ce_{1-x}La_xRu_2Si_2$ AF alloy with $x=0.2$.[22] In the latter,

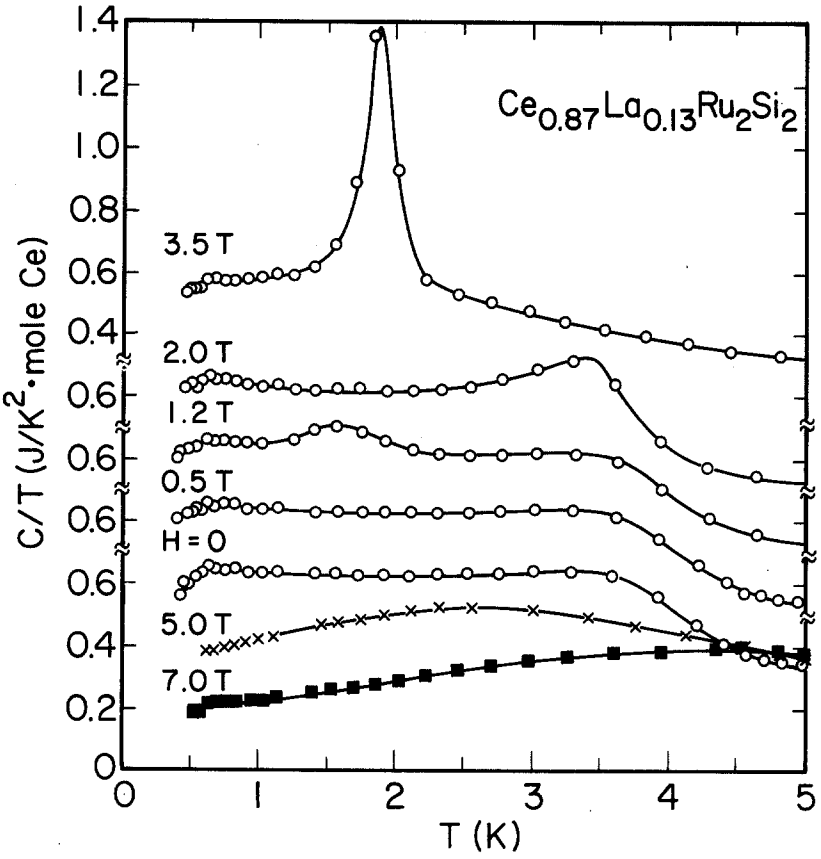

Fig. 27. Data of Fig. 26 for $T \leq 5$ K, replotted as C/T versus T.

where T_N is close to 6 K, a second phase transition is observed, for $H < H_a$, at a temperature T_L close to 2 K. This transition is characterized, in particular, by an upturn of the third-order harmonic component $3k_1$ of the incommensurate propagation vector $k_1 = (0.309, 0, 0)$, which characterizes the AF ordering below T_N. It is interpreted as a squaring of the modulated structure, and it leads to anomalies in the electrical resistivity and in the thermal dilation (see Ref. 22 and other references therein). In the present case the value of T_L might be as low as 0.6 K. Still, according to Ref. 22, the H_a line is not exactly horizontal but shows a rounded maximum. The existence of two anomalies in the present case, at 0.6 and 1.55 K for $H = 1.2$ T, can thus be explained as two crossings of this line. The two kinks occurring in C/T at 0.65 K for $H = 2$ and 3.5 T could be a manifestation of a quasivertical line

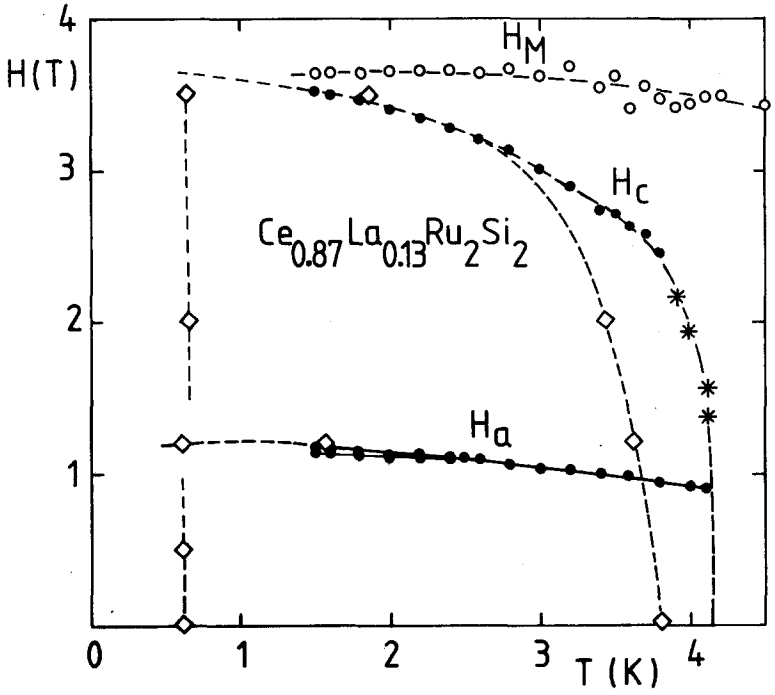

Fig. 28. Low-temperature H-T phase diagram for $x=0.13$. Data points derived from: M versus H measurements at constant T (● and ○); M versus T measurements at constant H (∗); specific-heat anomalies (◇).

in the $H_a < H < H_c$ region, which again by analogy to that reported for $x=0.2$, might correspond to a change in the modulated structure.

6. DISCUSSION

6.1. General Remarks

No attempt will be made to fit the data with a phenomenological model using a Lorentzian density of states that can be shifted from the Fermi level in zero field in order to reproduce metamagnetic transitions, and/or maxima in the temperature variation of C/T, since only crude adjustments can be obtained (see Refs. 7, 23, 24). We will focus (mainly) on the temperature variations of the specific heat and C/T and make comparisons with other heavy-fermion compounds.

A striking feature of the results is that Fig. 13 that reproduces, at $H=0$, the different behaviors characteristic of PP ground states, $x=0$ and 0.05,

and AF ground states, $x=0.1$ and 0.13, is rather similar to Fig. 26, which represents the AF case $x=0.13$ for different applied fields; the curves of Fig. 26 for $x=0.13$ at $H=5$ and 7 T resemble those of Fig. 13 at $H=0$ for $x=0.05$ and $x=0$, respectively. For $x=0.13$, the specific-heat anomaly at T_N is rather similar to that of the archetypical magnetically ordered Kondo compound $CePb_3$.[25]

The extrapolation of $\gamma(H) \equiv C/T$ to $T=0$ as a function of H is shown in Fig. 29. There is a sharp enhancement of γ as $H \to H_M$ for PP systems. As noted above, this enhancement is 28% for $x=0.05$. The latter experimental value is in excellent agreement with the enhancement deduced by the application of the Maxwell relation $(\partial\gamma/\partial H)_T=(\partial^2 M/\partial T^2)_H$ to magnetization data that show a T^2 behavior of M below ~ 1 K.[26] For $x=0$, an enhancement of γ up to 62% at H_M can be deduced in the same way from magnetization measurements.[27,28] it is interesting to compare the above estimates with those derived from magnetoresistance experiments. For $x=0$, the measurements of Ref. 1, predict an enhancement of the order of 50% assuming the coefficient A of the AT^2 term of the resistivity scales as γ^2. On warming, ρ changes from a quadratic AT^2 to a linear BT law, and B may scale directly

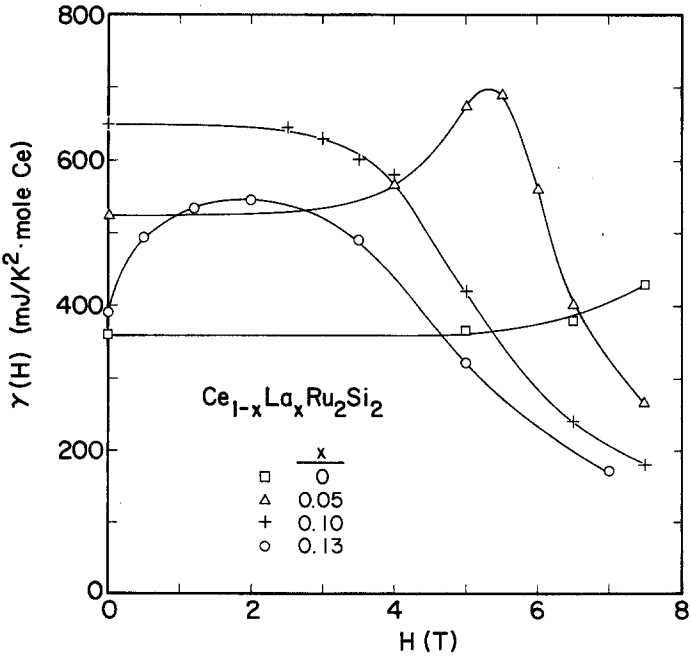

Fig. 29. $\gamma(H)$ versus H for different x. $\gamma(H)$ is the extrapolated value of C/T at $T=0$.

as γ. However, in the range $1.5 \leq T \leq 4.2$ K these measurements show an increase of the coefficient B of the BT term of only 30%. For an $x = 0.05$ alloy, an increase of B of 15% has been observed.[29] Thus, in both cases, the enhancement of γ, derived either directly or from low-temperature magnetization experiments, is about twice that predicted by that of B, while the enhancement of A (~ 2.4) is of the right order. For $H \sim H_M$, the low temperature regime [$T < T^*$ or $T < T(\alpha_{max})$] is reached only at very low temperature. At H_M, $T(\alpha_{max}) \sim 500$ mK.[28]

By contrast, for the AF case, $x = 0.1$, no enhancement of γ seems to occur at H_c. The further decrease of $\gamma(H)$ at $H > H_c$ is similar to that of the PP case $x = 0.05$. For the archetypical AF heavy-fermion compound $CeAl_2$, which has a metamagnetic transition at $H_c \sim 5$ T,[30] no evidence of enhancement of γ as H approaches H_c was observed. A careful study[31] of the temperature dependence of the magnetoresistivity of $CeAl_2$, leading to the field variation of $A(H)$, the coefficient of the T^2 term in the resistivity, confirms this absence of any enhancement of γ at H_c. In CeB_6, another well-known AF heavy-fermion compound, an enhancement of γ has been found,[32] but it corresponds to a transition between two ordered magnetic phases.

On the other hand, for $x = 0.13$, there is an enhancement of γ with increasing H at low field. This might be due to the fact that for this alloy the data extend far enough below T_N. At $H = 0$, a kink is observed in C/T at 0.6 K, which, as already mentioned, may correspond to the temperature T_L, where a squaring of the modulated structure should occur. Figure 14 shows the onset of a drastic decrease of γ from ~ 640 mJ mole^{-1} K^{-2} just above T_L to a value that might be as low as ~ 390 mJ mole^{-1} K^{-2} for $T = 0$. For $0 < H < H_c$, higher γ values are obtained (although lacking in accuracy because of the difficulty in extrapolating C/T to $T = 0$ below the kinks at 0.6–0.65 K, see Fig. 27). The increase in γ seems to be related, as in the case of CeB_6, to the existence of different magnetic structures below H_c. It may be concluded that as for the AF cases, $x = 0.1$ or $CeAl_2$, no enhancement of γ occurs at H_c for $x = 0.13$. Finally, a large decrease of $\gamma(H)$ is also observed above H_c.

6.2. Pure Compound $x = 0$. A Magnetic Instability at $T = 0$ for $H \to H_M$

The enhancement of γ for a (PP) ground state at H_M coincides with the decrease of intersite coupling as detected by the vanishing of the antiferromagnetic correlations. One possibility is that just for $H = H_M \pm \varepsilon$, the ferromagnetic component (wavevector $q \to 0$) plays a dominant role in the sharp increases of γ. The increase of the ratio $\chi(H)/\gamma(H)$ at H_M by roughly one order of magnitude at $T \to 0$ K[28] may point out the importance of ferromagnetic fluctuations. However, this value is taken at constant pressure P.

Another drastic variable is the volume; the huge magnetostriction at H_M may be responsible for the strong increase of $\chi(H)$ at constant volume that can demonstrate that, without volume change, the enhancement of χ/γ at H_M will be large.

A major parameter is the volume and its change induced under pressure and magnetic field. A striking point is that a collection of the maxima of the amplitudes reached by γ in the isostructural compounds $Ce_{1-x}La_xRu_2Si_2$, $CeRu_{2-x}Rh_xSi_2$[34] or $CeRu_2Si_{1-x}Ge_x$[15] leads to a quasiconstant value $(\gamma_c) \sim 600$ mJ mole^{-1} K^{-2} with deviations of 10% [for $CeRu_2Si_2$ $\gamma(H_M) = 563$ mJ mole^{-1} K^{-2}, for $Ce_{0.95}La_{0.05}Ru_2Si_2$ $\gamma(H_M) = 655$ mJ mole^{-1} K^{-2}]. That suggests that γ_c is a critical value characteristic of the instability between long-range magnetic ordering and Pauli paramagnetism. A simple picture is that the magnetic field induces a large volume change which almost drives the system to a magnetic phase transition at H_M with $T_N(H_M)$ close to zero.

For $H > H_M$, it is clear that the ground state is a polarized Pauli paramagnet. For $H < H_M$, one might wonder about the possible existence of small, ordered magnetic moments, but up to now there has been no experimental evidence for the occurrence of weak antiferromagnetism in $CeRu_2Si_2$. The specific-heat measurements in fields up to 13 T at 1.5 K reported[15] for a polycrystalline sample of $CeRu_2Si_2$ confirm qualitatively some features reported here: the emergence of a maximum in C/T at H_M and the rapid drop of C/T above H_M. Magnetization experiments performed on a single crystal up to 15 T have shown[9] that for this field γ decreases to 145 mJ mole^{-1} K^{-2}. Recent measurements[35] performed up to 20 T for $H//c$ on the $x=0$ single crystal of ref. 9 show at 1.5 K a maximum of C/T at H_M close to the expected value.[28] Then for $H=20$ T, C/T decreases to 80 mJ mole^{-1} K^{-2}.

Our results show that $CeRu_2Si_2$ is near the borderline of a magnetic instability as demonstrated, i) by the emergence of AF ordering on substitution of lanthanum ions for the cerium ions, and ii) the possibility of approaching the magnetic instability with a magnetic field. The energy scale, as defined by $T(\alpha_{max})$,[21,28] which is near 10 K at $H=0$, drops by at least an order of magnitude at H_M. This is now well established by susceptibility, magnetization, thermal expansion, magnetostriction,[26,28] and also by ultrasonic[12] and thermoelectric power[36] measurements. Although the effects are less spectacular in specific-heat measurements, there is also clear evidence of a low-energy scale for H approaching H_M. An interesting feature is that for $x=0$ a maximum in C/T emerges at low temperatures as H reaches the vicinity of H_M (see Figs. 21 and 22 and ref. 35). Such an effect is not observed in the $x=0.05$ PP alloy (Fig. 22a). Clearly, alloying destroys the anomaly of the pure system for which there is translation invariance. The interesting

point is that the occurence of AF ordering restores magnetically a coherence initially destroyed by alloying.

6.3. AF Cases

Neutron experiments (performed for $x=0.20$)[37] show the coexistence of strong magnetic fluctuations together with the incommensurate long-range order below T_N. Experiments performed in magnetic fields[22] show that with changing H, transitions can be induced easily between the $H=0$ incommensurate phase with propagation vector k_1, the commensurate phase with propagation vector (1/3, 1/3, 0) and the other incommensurate phase with propagation vectors k_1 and $k_2=(0.309, 0.309, 0)$. For the wavevectors k_1 and k_2, AF correlations are detected in the pure compound.[4]

It is of interest to understand the role of La substitution in the incomplete formation of AF order since neutron experiments at $x=2$ show that the correlation length does not diverge at T_N but only increases sharply from 30 Å at $T_N \sim 5.8$ K to 200 Å at 1 K.[37] This behavior may be a simultaneous result of the proximity of the magnetic instability and the high sensitivity of the electronic characteristic energy (the Kondo temperature) to the molar volume.[2,3] The inhomogeneity of the sites (differences in molar volume and local environment) may lead to drastic effects in the full establishment of the AF ordering. It is obvious that experiments on the pure compound are the most relevant. The non divergence of the coherence length at T_N must be clarified in the case of a pure lattice located just on the AF side of the magnetic instability.

6.4. Comparison with Other Heavy-Fermion Compounds: UPt_{3-x}, $CeAl_3$

The results presented here are of interest as a contribution to the development of a systematic description of a heavy-fermion compound that presents a strong interplay between intersite coupling and local fluctuations. Similar conditions are realized in UPt_3 doped with Pd or Th,[38] but the experimental difficulty is that the magnetic fields are far higher (~ 21 T) in pure UPt_3 and above 15 T in the alloys. Basically, the major phenomenon, an enhancement of γ at H_M that is very weak by comparison with the maximum of χ, is also observed.[39,40] The difference is that it has been proven by neutron diffraction that the pure compound, UPt_3, is AF ordered with a small moment, $10^{-2}\mu_B$, at $T_N=5$ K.[41,42] A striking feature is the broadening of the magnetic reflection by comparison with the nuclear Bragg peaks. That may be due to the difficulty of reaching a low concentration of stacking faults, as emphasized by the strong dependence of the electronic parameters on molar volume. Another interesting possibility is that the broadening reflects an intrinsic finite coherence length, i.e., the incompleteness of the

AF ordering: the interference effects may be suppressed by diffraction phenomena due to residual fluctuations even at zero frequency. Careful specific-heat and susceptibility measurements do not detect any indication of magnetic ordering. Until now, no AF reflection has been observed in $CeRu_2Si_2$. It should be stressed that, as suggested by the behavior of $CeRu_2Si_2$, inducing a well-localized magnetic ordering in UPt_3 by doping may be the consequence of producing an entirely new situation rather different from the pure lattice, since in $UPt_{3-x}Pd_x$ the Néel temperature has almost the same value while the sublattice magnetization is two orders of magnetiude higher for $x=0.03$ than for $x=0$.[41,43] The similarity between pure and doped materials would then be only apparent. To study the itinerant nature of the magnetism, systematic studies must be made for $x\to 0$. Experimentally, there is now a need for improvement of sample quality, i.e., for example, a systematic study of the influence of the disorder (i.e., inversion of the Ru and Si sites, relation between residual resistivity and specific heat or magnetization anomalies).

$CeAl_3$ was considered for more than a decade as a PP.[44] The discovery of a spontaneous Larmor precession frequency in μSR experiments below 0.7 K; the simultaneous observation of muon-spin relaxation below 2 K[45]; the observation of the Al NMR line broadening below 1.2 K[46] and, as well, the occurrence of drastic changes in magnetoresistivity and temperature dependence of the resistivity below 1.6 K[47] were interpreted as showing the

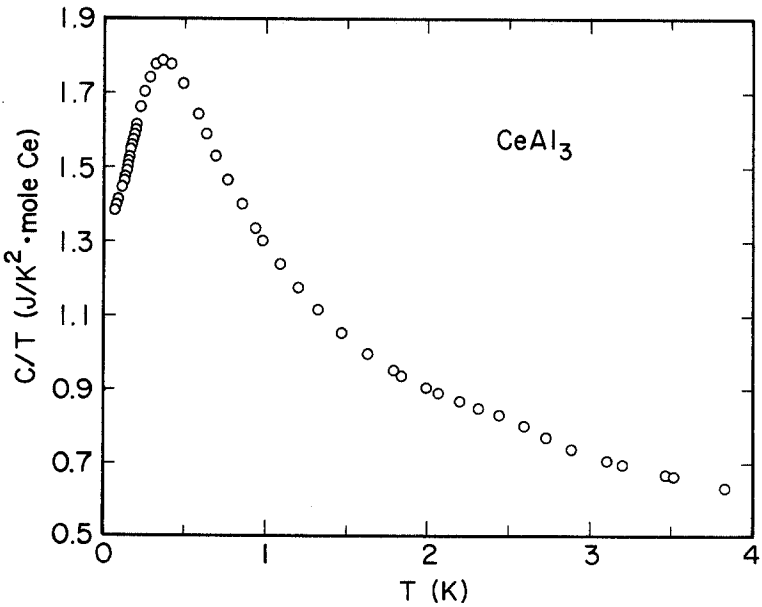

Fig. 30. C/T versus T for $CeAl_3$.

onset of static magnetic correlations. NMR and muon experiments give, respectively, a value of $0.3\mu_B$/Ce for the maximum of a static moment on Ce sites, and a lower limit of 0.1 μ_B/Ce. The puzzle is that no clear evidence of a specific-heat anomaly can be found. By analyzing the temperature variation of C/T, a maximum of $C/T \sim 1.8$ J mole^{-1} K^{-2} appears at $T \sim 0.35$ K with an amplitude 20% higher than the extrapolated limit at $T=0$[48–50] (Fig. 30) No inflection point in C/T can be detected near 1.6 K; however, a small anomaly in C/T appears at $T \sim 2.5$ K. Before claiming an intrinsic origin for this weak bump, due to the difficulty of avoiding the parasitic phases Ce_3Al_{11} and $CeAl_2$, systematic measurements on different samples are needed. By comparison, in $Ce_{1-x}La_xSi_2$, for $x=0.1$ and $x=0.13$ inflection points in C/T occur at 2.9 and 4.3 K with maxima at 2 and 3.5 K, respectively. As noted above, in this case the inflexion point corresponds well to T_N. It was emphasized for $CeAl_3$ that, from an analysis of muon data, the coherence length may be very short and furthermore the new ordered phase appears below 2 K in a static inhomogeneous frustrated way[51] reminiscent of a spin-glass behavior. This statement may be consistent with the linear temperature decrease of C/T on cooling below its maximum at 0.35 K as observed for typical spin glasses such as Cu Mn.[52] It seems that the interplay between intrinsic and extrinsic properties is strong in $CeAl_3$, which is just at the edge of a magnetic instability.[53] However, the large temperature range in which C/T increases on cooling is certainly not governed by imperfections in the crystal since samples prepared in different laboratories have quite similar specific heats.[54] None of the different curves measured here for $Ce_{1-x}La_xRu_2Si_2$ reproduces the behavior of $CeAl_3$ which may, however, be realized for pure $CeRu_2Si_2$ at negative pressure or perhaps under uniaxial stress.

7. CONCLUSION AND THEORETICAL MODELS

The present studies on $Ce_{1-x}La_xRu_2Si_2$ demonstrate the unique situation of the pure lattice ($x=0$), i.e., the role of the itinerant character of the heavy electrons. A sharp enhancement of γ, i.e., of the effective mass, at H_M appears to occur here only for the PP ground state. In the ordered systems, $x=0.1$ and 0.13, the magnetic correlations, detected for example by the occurrence of a well-defined maximum $\chi(H_M)$ at H_M, collapse in the paramagnetic regime only at low temperature, far below the ordering temperature. It is worth emphasizing that also for the typical heavy-fermion compounds UPt_3 and $CeAl_3$, which present static magnetic correlations at $H=0$, the behavior cannot be extrapolated from alloying studies. Their respective enhancements of γ at metamagnetic-like transitions seem to have no correspondence with features of magnetically ordered heavy-fermion compounds

(CeB_6, $CeAl_2$) at their transitions under magnetic field to polarized paramagnetic phases.

The main theoretical ingredient of any model seems to be competing local fluctuations and intersite coupling, and the feedback to the lattice spacing. It is also clear that the itinerant nature of the quasiparticles is crucial. That leads to the idea that the occurrence of small ordered moments and metamagnetism in heavy-fermion compounds are closely connected. Three different theoretical approaches have been proposed recently for the metamagnetism in heavy-fermion compounds.

The first, referred to as the Kondo volume-collapse model,[34], is based on a ferromagnetic molecular field, and a large Grüneisen parameter with a feedback between the magnetization and the lattice spacing. Its strength is in showing the interplay between magnetism and volume change. Its weakness, connected with use of the molecular-field approximation, is the impossibility of finding a large enhancement of γ at H_M: only a shallow maximum is found, and furthermore it is not at H_M.

Secondly, in a model of weakly interacting Kondo centers,[55] magnetization processes like metamagnetism have been reproduced qualitatively. Treating the intersite correlations beyond the mean-field level shows that the intersite correlations themselves depend on the magnetization.

Finally, a new quantum phenomenological model[56] has been formlated for heavy-fermion systems in order to take into account simultaneously the localized spin-fluctuation contribution and the itinerant-fermion quasiparticles. Metamagnetism as well as weak antiferromagnetism are qualitatively explained. For example, the experimental observation that $\chi_0 H_M$ is pressure invariant is found; such a simple scaling law is not found in the first appraoch or in the usual spin-fluctuation models. The field enhancement of γ at H_M has not yet been calculated in either of the two latter approaches.

ACKNOWLEDGEMENTS

We are grateful to J. M. Mignot for help with some of the measurements and for valuable discussions. A critical reading of the manuscript by R. Tournier and his suggestions for improvements were very helpful. The work at Berkeley was supported by the Director, Office of Energy Research, Office of Basic Energy Sciences, Materials Sciences Division of the U.S. Department of Energy under contract number DE-ACO3-76SF00098.

REFERENCES

1. P. Haen, J. Flouquet, F. Lapierre, P. Lejay, and G. Remenyi, *J. Low Temp. Phys.* **67**, 391 (1987).

2. J. M. Mignot, J. Flouquet, P. Haen, F. Lapierre, L. Puech, and J. Voiron, *J. Magn. Magn. Mater.* **76&77**, 97 (1988) and references therein.
3. I. Kouroudis, D. Weber, M. Yoshizawa, B. Lüthi, L. Puech, P. Haen, J. Flouquet, G. Bruls, U. Welp, J. J. M. Franse, A. Menovsky, E. Bucher, and J. Hufnagl, *Phys. Rev. Lett.* **58**, 820 (1987).
4. J. Rossat-Mignod, L. P. Regnault, J. L. Jacoud, C. Vettier, P. Lejay, J. Flouquet, E. Walker, D. Jaccard, and A. Amato, *J. Magn. Magn. Mater*, **76 & 77**, 376 (1988).
5. S. Quézel, P. Burlet, J. L. Jacoud, L. P. Regnault, J. Rossat-Mignod, C. Vettier, P. Lejay, and J. Flouquet, *J. Magn. Magn. Mater.* **76 & 77**, 403 (1988).
6. J. L. Tholence, P. Haen, D. Jaccard, P. Lejay, J. Flouquet, and H. F. Braun, *J. Appl. Phys.* **57**, 3172 (1985).
7. (a) M. J. Besnus, J. P. Kappler, P. Lehmann, and A. Meyer, *Solid State Commun.* **55**, 779 (1985); (b) M. J. Besnus, P. Lehmann, and A. Meyer, *J. Magn. Magn. Mater.* **63 & 64**, 323 (1987); (c) P. Lehmann, thesis, Université Louis Pasteur, Strasbourg (1987).
8. (a) P. Haen, F. Lapierre, J. P. Kappler, P. Lejay, J. Flouquet, and A. Meyer, *J. Magn. Magn. Mater.* **76 & 77**, 143 (1988); (b) P. Haen, J. P. Kappler, F. Lapierre, P. Lehmann, J. Flouquet, P. Lejay, and A. Meyer, *J. Phys. (Paris)* **49**, (Suppl.) C8-757 (1988); (c) P. Haen, J. Voiron, F. Lapierre, J. Flouquet, and P. Lejay, *Physica B* **163**, 519 (1990).
9. A. Lacerda, A. de Visser, L. Puech, P. Lejay, P. Haen, J. Flouquet, J. Voiron, and F. J. Ohkawa, *Phys. Rev. B* **40**, 11429 (1990).
10. R. A. Fisher, N. E. Phillips, C. Marcenat, J. Flouquet, P. Haen, P. Lejay, and J. M. Mignot, *J. Phys.* **49** (Suppl.), C8-759 (1988).
11. L. Puech, J. M. Mignot, J. Voiron, P. Lejay, P. Haen, and J. Flouquet, *J. Low Temp. Phys.* **70**, 237 (1988).
12. G. Bruls, D. Weber, B. Lüthi, J. Flouquet, and P. Lejay, *Phys. Rev. B.* **42**, 4329 (1990).
13. F. Steglich, U. Rauchschwalbe, U. Gottwick, H. M. Mayer, G. Spain, N. Grewe, U. Poppe, and J. J. M. Franse, *J. Appl. Phys.* **57**, 3054 (1985).
14. J. D. Thompson, J. D. Willis, C. Godart, D. E. MacLaughlin, and L. C. Gupta; *Solid State Commun.* **56**, 169 (1985).
15. J. S. Kim, B. Andraka, G. Fraunberger, and G. R. Stewart, *Phys. Rev. B* **41**, 541 (1990).
16. A. Severing, E. Holland-Moritz, and B. Frick, *Phys. Rev. B* **39**, 4164 (1989).
17. L. P. Regnault and J. M. Mignot, private communication.
18. Y. Lassailly, S. K. Burke, and J. Flouquet, *J. Phys.C* **18**, 5737 (1985).
19. J. Flouquet, P. Haen, and C. Vettier, *J. Magn. Magn. Mater.* **29**, 159 (1982).
20. A. Amato, D. Jaccard, J. Flouquet, F. Lapierre, J. L. Tholence, R. A. Fisher, S. E. Lacy, J. A. Olsen, and N. E. Phillips, *J. Low Temp Phys* 68, 371 (1987).
21. A. Lacerda, A. de Visser, L. Puech, P. Lejay, P. Haen, and J. Flouquet, *J. Appl. Phys.* **67**, 5212 (1990).
22. J. M. Mignot, J. L. Jacoud, L. P. Regnault, J. Rossat-Mignod, P. Haen, P. Lejay, Ph. Boutrouille, B. Hennion, and D. Petitgrand, *Physica B* **163**, 611 (1990); J. M. Mignot, L. P. Regnault, J. L. Jacoud, J. Rossat-Mignod, P. Haen, and P. Lejay, Sixth ICVF, Rio de Janiero, July 1990 (to be published in *Physica B*).
23. C. D. Bredl, F. Steglich, and K. D. Schotte, *Z. Phys. B* **29**, 327 (1978); C. D. Bredl, thesis, Darmstadt (1980).
24. J. Flouquet, P. Haen, C. Marcenat, P. Lejay, A. Amato, D. Jaccard, and E. Walker, *J. Magn. Magn. Mater.* **52**, 85 (1985); C. Marcenat, Thesis, Grenoble (1986).
25. C. L. Lin, J. Teter, J. E. Crow, T. Mihalisin, J. Brooks, A. I. Abou Ali, and G. R. Stewart, *Phys. Rev. Lett.* **54**, 2541 (1985).
26. C. Paulsen, A. Lacerda, A. de Visser, K. Bakker, L. Puech, and J. L. Tholence, *J. Magn. Magn. Mater.*, **90 & 91**, 408 (1990).
27. C. Paulsen, A. Lacerda, J. L. Tholence, and J. Flouquet, *Physica B* **165-166**, 433 (1990).
28. C. Paulsen, A. Lacerda, L. Puech, P. Haen, J. L. Tholence, P. Lejay, J. Flouquet, and A. de Visser, *J. Low Temp. Phys.* **81**, 317 (1990); A. Lacerda, thesis, Université Joseph Fourier, Grenoble (1990).
29. R. Djerbi, thesis, Université Joseph Fourier, Grenoble (1989); R. Djerbi, P. Haen, F. Lapierre, and J. M. Mignot, *J. Magn. Magn. Mater.* **76 & 77**, 265 (1988).

30. B. Barbara, M. F. Rossignol, H. G. Purwins, and E. Walker, *Solid State Commun.* **17**, 1525 (1975).
31. K. Behnia, private communication.
32. C. Marcenat, R. A. Fisher, N. E. Phillips, and J. Flouquet, *J. Magn. Magn. Mater.* **76 & 77**, 115 (1988); T. Müller, W. Joss, U. van Ruitenbeek, U.Welp, P. Wyder, and Z. Fisk, *J. Magn. Magn. Mater.* **76&77**, 35 (1988).
33. F. J. Ohkawa, *Solid State Commun.* **71**, 907 (1989).
34. B. Lloret, B. Chevalier, B. Buffat, J. Etourneau, S. Quézel, A Lamharrar, J. Rossat-Mignod, R. Calemczuk, and E. Bonjour, *J. Magn. Magn. Mater.* **63 & 64**, 85 (1987); R. Calemczuk, E. Bonjour, J. Rossat-Mignod, and B. Chevalier, *J. Magn. Magn. Mater.* **90 & 91**, 477 (1990).
35. H. P. Van der Meulen, A. de Visser, J. J. M. Franse, T. T. J. M. Berendschot, J. A. A. J. Perenboom, H. van Kempen, A. Lacerda, P. Lejay, and J. Flouquet, *Phys. Rev. B* **44** (1991).
36. A. Amato, D. Jaccard, J. Sierro, P. Haen, P. Lejay, and J. Flouquet, *J. Low Temp. Phys.* **77**, 195 (1989).
37. L. P. Regnault, J. L. Jacoud, J. M. Mignot, J. Rossat-Mignod, C. Vettier, P. Lejay, and J. Flouquet, *Physica B* **163**, 606 (1990); L. P. Regnault, J. L. Jacoud, J. M. Mignot, J. Rossat-Mignod, C. Vettier, P. Lejay, and J. Flouquet, *J. Magn. Magn. Mater.* **90 & 91**, 398 (1990).
38. J. J. M. Franse, M. van Sprang, A. de Visser, and A. A. Menovsky, *Physica B* **163**, 511 (1990).
39. T. Müller, W. Joss, and L. Taillefer, *Phys. Rev. B* **40**, 2614 (1989).
40. H. P. van der Meulen, Z. Tarnawski, A. de Visser, J. J. M. Franse, J. A. A. J. Perenboom, D. Althof, and H. van Kempen, *Phys. Rev. B* **41**, 9352 (1990).
41. See G. Aeppli, E. Bucher, A. I. Goldman, G. Shirane, C. Broholm, and K. J. Kjems, *J. Magn. Magn. Mater.* **76 & 77**, 385 (1988).
42. L. Taillefer, *Physica B* **163**, 278 (1990); L. Taillefer, K. Behnia, K. Hasselbach, J. Flouquet, S. M. Hayden, and C. Vettier, *J. Magn. Magn. Mater.* **90 & 91**, 623 (1990).
43. A. I. Goldman, G. Shirane, G. Aeppli, B. Batlogg, and E. Bucher, *Phys. Rev. B* **34**, 6564 (1986).
44. K. Andres, J. E. Graebner, and H. R. Ott, *Phys. Rev. B* **35**, 1779 (1975).
45. S. Barth, H. R. Ott, F. N. Gygax, B. Hitti, E. Lippelt, A. Schenk, C. Baines, B. van den Brandt, T. Konter, and S. Mango, *Phys. Rev. Lett.* **59**, 2991 (1987).
46. H. Nakamura, Y. Kitaoka, K. Asayama, and J. Flouquet, *J. Magn. Magn. Mater.* **76 & 77**, 465 (1988).
47. D. Jaccard, R. Cibin, J. L. Jorda, and J. Flouquet, *Jpn. J. Appl. Phys.* **26**, 517 (1987).
48. J. Flouquet, J. C. Lasjaunias, J. Peyrard, and M. Ribault, *J. Appl. Phys.* **53**, 2127 (1982).
49. C. D. Bredl, S. Horn, F. Steglich, B. Lüthi, and R. M. Martin, *Phys. Rev. Lett.* **52**, 1982 (1984).
50. G. E. Brodale, R. A. Fisher, N. E. Phillips, and J. Flouquet, *Phys. Rev. Lett.* **56**, 390 (1985).
51. S. Barth, H. R. Ott, F. N. Gygax, B. Hitti, E. Lippelt, A. Schenk, and C. Baines, *Phys. Rev.* **39**, 11695 (1989).
52. W. H. Fogle, J. C. Ho, and N. E. Phillips, *J. Phys.* **39**, (Suppl.), C6-901 (1978).
53. Ch. Fierz, D. Jaccard, J. Sierro, and J. Flouquet, *J. Appl. Phys.* **63**, 3899 (1988).
54. J. Flouquet, P. Haen, P. Lejay, P. Morin, D. Jaccard, J. Schweizer, C. Vettier, R. A. Fisher, and N. E. Phillips, *J. Magn. Magn. Mater.* **90&91**, 377 (1990).
55. K. Ueda, K. Yamamoto, and R. Konno, *J. Magn. Magn. Mater.* **90 & 91**, 419 (1990).
56. K. Miyake and Y. Kuramoto, *J. Magn. Magn. Mater.* **90 & 91**, 438 (1990).